(NASA CR-55371;
~~Report No.~~ AE62-0092)
OTS:

STUDY OF PRINCIPLES OF METEOROID PROTECTION

by

R. F. Rolsten, H. H. Hunt, and J. N. Wellnitz

~~January~~ 1962

(NASA Contract NAS-8-875)
Progress Report No. 3, 2 Oct. - 29 Dec. 1961

X
[10]

RDF62-006

George C. Marshall Space Flight Center
National Aeronautics and Space Administration
Huntsville, Alabama

GENERAL DYNAMICS | ASTRONAUTICS, San Diego, Calif.

3517703

ABSTRACT

14899

Literature data pertinent to the phenomena associated with hypervelocity impact of relatively thin plates and the principles of meteoroid protection were given in Progress Report No. 1. The preliminary data resulting from the impact of a cylindrical steel projectile (approximately 15,000 ft/sec) on thin plates of aluminum (7075, 2024-T3 and 6061-T6), titanium (75-A) and magnesium alloy (HK-31A) were presented in Progress Report No. 2.

The progress made during this report period can be summarized as follows.

1. Additional impact data were obtained with the 0.090- and 0.063-inch aluminum (6061-T6) bumpers.

2. Impact data were obtained with 0.125- and 0.032-inch aluminum (6061-T6) bumpers.

3. Bumpers of plate glass and wire screen were tested.

4. The 0.57-gram projectile was accelerated, with slight premature fragmentation, to a velocity of 26,800 ft/sec.

5. Projectile mass was lowered to 0.097-gram.

6. Copper and glass projectiles were accelerated to high velocity (12,000 ft/sec).

7. The evaluation of energy absorbers was started.

8. Structures pressurized with water and gaseous oxygen were tested.

9. High speed photographic coverage of the impact phenomena were obtained.

10. The principles of meteoroid protection were elaborated further. Author

FOREWORD

This report was prepared by the Materials Research Group of General Dynamics/Astronautics on National Aeronautics and Space Administration Contract, NAS-8-875, "Study of Principles of Meteoroid Protection". The program is administered under the direction of Mr. Henry L. Martin of the Physics and Astrophysics Branch, Research Projects Division.

Drs. R. F. Rolsten and W. H. Steurer of General Dynamics/Astronautics are responsible for the study, organization and technical direction of the work performed. In addition to the forementioned, the principal contributors to this phase of the investigation are Messrs. H. H. Hunt, J. N. Wellnitz, J. E. Mathews and H. Anderson.

The report contains the results of the studies performed between 2 October and 29 December 1961.

TABLE OF CONTENTS

Section		Page
I.	Introduction	1
II.	Total Mass and Spacing to Prevent Penetration and/or Spallation	3
III.	Investigation of Bumper Effectiveness	7
	A. Solid Metal Bumper	7
	1. Aluminum Bumper, Type 6061-T6, 0.125-Inch Thick	7
	2. Aluminum Bumper, Type 6061-T6, 0.090-Inch Thick	7
	3. Aluminum Bumper, Type 6061-T6, 0.063-Inch Thick	8
	4. Aluminum Bumper, Type 6061-T6, 0.032-Inch Thick (0.57-Gram Steel Projectile)	8
	5. Aluminum Bumper, Type 6061-T6, 0.090-Inch Thick; Copper Projectile	8
	B. Glass Bumpers	9
	C. Wire Screen Bumpers	9
IV.	Principles of Meteoroid Protection	13
	A. Case I The Relatively Thin Single Plate	13
	B. Case II The Single Meteoroid Bumper	14
	C. Summary	15
V.	Low Mass Projectiles	17
VI.	Pressurized Structures	19
	A. Test Panel No. 1	19
	B. Test Panel No. 2	20
VII.	Energy Absorbers	21
VIII.	Projectiles	23
	A. Physical State	23
	B. Glass Projectiles	23
IX.	Photographic Analysis of Impact Phenomena	25
	A. Low Speed Photographs	25
	B. Moderate Speed Photographs	25
	C. High Speed Photographs	26
Appendix A	Projectile Orientation and Fragmentation	29

ILLUSTRATIONS

Figure		Page
1	Mass and Spacing to Prevent Penetration (0.125-Inch Bumper)	30
2	Mass and Spacing to Prevent Penetration (0.090-Inch Bumper)	31
3	Mass and Spacing to Prevent Penetration (0.063-Inch Bumper)	32
4	Mass and Spacing to Prevent Penetration (0.032-Inch Bumper)	33
5	Mass and Spacing to Prevent Penetration (Aluminum and Plate Glass Bumpers)	34
6	Craters Produced in Aluminum with Copper and Steel Projectiles	35
7	Vehicle Hull Protected with the 0.094-Inch Plate Glass Bumper	36
8	The Effect of Velocity on Penetration	37
9	Mass and Spacing to Prevent Penetration (0.032- to 0.125-Inch Bumper)	38
10	Liquid Pressurized Tank During Impact	39
11	Liquid Pressurized Tank After Impact	40
12	Gas Pressurized Tank During Impact	41
13	Oxygen Pressurized Tank: Test Panel No. 1	42
14	Oxygen Pressurized Tank: Test Panel No. 2	43
15	Burning of an Oxygen Pressurized Tank	44
16	Fiberglas Energy Absorber	45
17	MIN K-1300 Energy Absorber	46
18	Fibrous Potassium Titanate Energy Absorber	47
19	Honeycomb Panel No. 1	48
20	Honeycomb Panel No. 2 (Impact Delaminated Rear Facing from Core)	49
21	Penetration Dependence on Impact Velocity of Solid and Liquid Projectiles	50
22	Glass Projectile Damage to an Aluminum Panel	51
23	Damage to Aluminum Plates by a Caliber .30-06 Bullet	52
24	Slow Speed Impact Photographs	53
25	Impact Flash	54
26	Dynafax Photograph of Impact Phenomena Associated with Intermediate Speed Projectile	55
27	Aluminum Plates Used in Experiment D-155	56
28	Dynafax Photograph of the Impact Phenomena Associated with a High Speed Projectile	57
29	Aluminum Plates Used in Experiment D-157	58
29A	Aluminum Plates Used in Experiment D-157	59
30	Projectile Behavior on Flat Face Impact	60
31	Projectile Behavior on Edge Impact	61

TABLES

Number		Page
I	Summary of Impact Data	4
	(Bumpers Without Energy Absorbers; Steel Projectiles)	4
	(Bumpers With Energy Absorbers; Steel and Copper Projectiles)	5
II	Definition of Symbols Used in the Figures to Describe the Projectile Impact Conditions	6
III	Comparison of Craters in Aluminum Produced With a Copper and Steel Projectile	10

I. INTRODUCTION

Numerous investigations have been carried out during the past several years because of the obvious significance of meteoric particle damage to space vehicles. These investigations are, however, primarily concerned with the theory of hypervelocity impact and the experimental assessment of the related phenomena. On the other hand, designers have proposed several schemes and configurations for protecting vehicles from meteoric particles, partly supported by very isolated and inconsistent experimental data. A paucity of pertinent design information has resulted from the concentration of the research programs on the impact phenomena occurring between like materials and with semi-infinite* plates; a simplification used to reduce the number of variables in a very complex system.

Theory and design have generally followed separate paths and presently, there are only a few attempts being made to integrate theoretical concepts and recognized phenomena in the development of structural systems. The prime prerequisite for the establishment of realistic design criteria is a systematic experimental research investigation, carried out on materials and structural configurations that are useful in actual vehicle design; such a systematic approach is being conducted in this research program. The approach selected in the presentation of the results will permit an expeditious alteration and revision when new environmental or other parametric data become available.

From the standpoint of the meteoroid bumper concept, a space vehicle structure is composed of three components: 1) the void (or material sandwiched) between, 2) the main hull, and 3) the meteoroid bumper. The bumper must be capable of fragmenting the meteoric particle and dispersing its energy over a larger area of the main hull, the sandwich material (if used) may reduce the damage from spall, and the main hull must have sufficient strength to transfer the momentum of the impacting particles without being penetrated. Actually, the three components function as an entity, but for the analysis of engineering materials during hypervelocity impact, each component must be considered phenomenologically.

In the previous progress report, primary emphasis was placed on the interaction between projectile and bumper and to the establishment of numerical data on the significance of total mass and spacing. The purpose of the present progress report is to refine the preliminary data and to develop tentative concepts into a synthesis of the individual relationships in order to provide an optimum minimum-weight protection system. This in turn, required the establishment of additional parametric data on the projectile composition, projectile mass, bumper material and structure, energy absorbing filler materials, and on the behavior of pressurized hulls. High speed photography equipment has been utilized in order to study the phenomena occurring prior to, during, and after impact.

---

* A semi-infinite plate has sufficient thickness to eliminate all free surface effects.

II. TOTAL MASS AND SPACING TO PREVENT PENETRATION AND/OR SPALLATION

The aluminum (6061-T6) bumper and vehicle hull* were subjected to normal impact from explosively accelerated projectiles with a velocity of approximately 15,000 ft/sec. Criteria for a satisfactory bumper-hull and mass-distance arrangement were based on the vehicle hull not being penetrated or cracked; i.e., the hull plate must be capable of maintaining gas pressure after impact.

In order to investigate only the bumper mass and separation distance, four bumper thicknesses (0.125-, 0.090-, 0.063- and 0.032-inch) were used. The distance of separation for any given total mass per unit area was increased until the test panel did not crack on impact. Pertinent data are summarized in Table I** and Figures 1 through 5 and 7. Definition of the symbols*** used in the figures are summaried in Table II. For example, experiment J-20 designated ABB, indicates that the projectile: A, struck the target nearly flat, B, fragmented to a slight extent before contacting the bumper and B, had an impact velocity in the range of 12,000 to 16,000 ft/sec. Although the desired impact conditions are AAC or AAD, it should be observed that conditions corresponding to BAC or BAD are more severe.

---

* The test panel is comprised of a bumper and the main wall of the vehicle hull.

** Table I in this report is a continuation of the data given in Table 1 of Report No. 2.

*** Note that the symbols designating the velocity limits for the reliability code given in Report No. 2 have been modified (by direction) in this Report.

Table I. Summary of Impact Data*

ROUND NO	REL CODE**	WT CHARGE (gms)	WT PROJECTILE (gms)	VELOCITY Ft Sec^{-1}	MOMENTUM Ft Lbs - Inch^{-2} Sec^{-1}	BUMPER THICKNESS (Inches)	SPACING (Inches)	TARGET PLATE THICKNESS	TOTAL WEIGHT Lbs Ft^{-2}	HOLE DIA. BUMPER (Inches)	SPRAY CONE DIA. (Inches)	PRINCIPLE CONE DIA. (Inches)	VEHICLE HULL PLATE PENETRATED (Depth)	VEHICLE HULL PLATE CRACKED	REMARKS
O-78	CCB	399.6	0.5835	14,300	-	0.125	0.5	0.625	10.63	0.4x0.48	0.9	≤ .5	No. 0.2"	No	Crater 0.5" dia. Slight bulge rear surf
O-79	CBB	400.4	0.5835	15,800	-	0.125	0.5	0.625	10.63	0.35x0.52	1.0	≤ .4	No. 0.37"	No	Crater 0.4" dia. Slight bulge rear surf
O-80	CAB	401.2	0.5850	15,600	-	0.125	1.0	0.50	8.87	0.4x0.48	1.4x1.6	-	Yes	-	0.35" dia. perforation - Spall 0.8" dia x 0.1" thick
S-81	CBC	400.6	0.5745	16,400	-	0.125	2.25	0.375	7.05	0.56x0.62	3	1.5	Yes	-	0.25" x 0.31" puncture
O-65	AAB	400.9	0.5702	12,500	320	0.090	3.0	0.375	6.57	0.35	5.0	1.0	Yes	-	0.7" dia. puncture. 0.15" thick x 1.1" dia. spall
O-90	BBB	397.9	0.5715	15,200	-	0.090	3.25	0.4375	7.456	0.27x0.42	4.0	.5" x 5"	Yes	-	0.3" dia. puncture
O-91	-	400.0	0.5750	-	-	0.090	3.25	0.4375	7.456	0.4	4.0	.8" x 1.4"	Yes	-	0.5" dia. puncture
O-64	ABC	392.1	0.5652	15,900	483	0.090	5.0	0.25	4.51	0.45	5.0	1" x 1.4"	Yes	-	2 - 0.375" and 1 - 0.25" dia. perforations
O-[illegible]	CCB	395.2	0.5650	13,500	-	0.050	6.06	0.3125	5.714	0.3x0.44	6.0	0.6x1.0	Yes	-	0.5" x 0.75" puncture Spall 0.75" dia x 0.05" thick
O-66	ABB	398.6	0.5845	14,800	389	0.063	0.25	0.75	11.484	0.56	-	-	No 0.42	No	0.82" x 0.94" dia crater. 0.05" high bulge
O-81	CCC	407.6	0.5748	17,200	-	0.063	0.25	0.75	11.484	-		-	No	No	Pellet broke into 5 parts
O-82	BCC	409.1	0.5778	16,200	-	0.063	0.25	0.75	11.484	0.28x0.37	0.5	-	No 0.36"	No	Crater 0.5" dia., lip 0.08" - Bulge 0.03" high
O-86	AAB	407.0	0.5832	14,300	375	0.063	1.0	0.562	8.918	0.44	1.9	1.2	No 0.25	No	Crater 1.15" dia. Bulge 0.04" high
O-87	CAB	395.3	0.5846	14,700	-	0.063	1.0	0.562	8.918	0.53x0.58	3.0	1.6 x 1.1	No	No	
O-89	BCB	400.8	0.5730	15,200	-	0.063	6.06	0.3125	5.338	0.3 x 0.37		0.5 x 1.9	Yes	-	0.5" x 0.65" diameter puncture
O-70	BAB	399.2	0.5835	14,100	-	0.032	0.25	0.75	11.032	0.12 x 0.4	0.6	-	Yes	-	0.55" dia. puncture - Spall 0.85" dia x 0.15" thick
O-71	ABC	402.0	0.5835	16,100	422	0.032	0.25	0.75	11.032	0.47	0.9	-	No. 0.52	No	Crater 0.[illegible]" dia., lip 0.08", Bulge 0.05" high
O-69	BBC	402.2	0.5837	18,100	-	0.032	1.0	0.625	9.322	0.3 x 0.4	-	-	Yes	-	Tapered 0.6" to 0.35" dia puncture
O-72	BBB	403.0	0.5838	14,300	-	0.032	1.0	0.625	9.322	0.2 x 0.35		-	Yes	-	Tapered 0.75" to 0.4" x 0.7", Spall 0.4" x 0.85" x 0.15" thick
O-75	AAB	402.6	0.5845	14,300	390	0.032	1.0	0.625	9.322	0.4 x 0.45	1.1 x 1.3	0.4 x .65	No. 0.35"	No	Crater 0.4" x 0.65", Bulge 0.08" high
S-96	BBB	402.2	0.5845	14,000	-	0.032	2.0	0.500	7.562	0.14 x 0.3[illegible]	0.8	0.7	Yes	-	0.6" dia. puncture Spall .8" dia. x .1" thick
S-97	ABB	402.3	0.5855	14,300	378	0.032	2.0	0.500	7.562	0.4 x 0.[illegible]	2.0	0.55 x 1.3	No. 0.35"	No	0.05" high bulge
S-54	ABC	399.4	0.5650	16,100	411	0.032	3.0	0.375	5.742	0.5	1.6	0.5	Yes	-	Spall 0.7" dia. x 0.1 thick
O-74	BAB	404.2	0.5853	15,100	-	0.032	4.0	0.375	5.742	0.25 x 0.4[illegible]	-	-	Yes	-	0.6" x 0.7" dia puncture
O-83	CC	403.1	0.5790	-	-	0.032	4.0	0.375	5.742	0.33	-	-	No	No	4 holes in bumper
O-84	CCD	406.[illegible]	0.5750	20,000	-	0.032	4.0	0.375	5.742	0.3[illegible] x 0.4	-	-	No	No	Moderate pellet breakup
O-85	CCB	395.5	0.5845	15,200	-	0.032	4.0	0.375	5.742	0.32 x 0.4	4	8	Yes		0.44" dia hole - Spall 0.[illegible]" dia x 0.1 thick
O-61	D	402.3	0.5845	20,000	-	0.094" window glass	0.5	0.625	10.03	-	1.[illegible]	1.7	No	No	Bulge 0.03"
O-60	C	402.8	0.5837	17,500	-	0.094" window glass	1.5	0.5	8.25	-	1	5	No 0.4	No	Main Crater 0.5" dia. Bulge 0.094 high
O-58	B	395.6	0.5835	14,700	-	0.094" window glass	2.5	0.375	6.43	-	5	0.5 x 1.4	Yes	-	0.3" dia. hole Bulge area 0.5 x 1.5
O-59	B	401.1	0.5840	13,500	-	0.094" window glass	3.0	0.375	6.43	-	[illegible] x 4	-	Yes	-	0.25 dia. puncture
O-94	ABB	404.7	0.5750	15,200	394	2 layers Al screen 0.028" 16 mesh	1.0	0.625	9.436	1st Scr 0.45 2nd Scr 0.3[illegible]	1.[illegible]	0.75	No. 0.47"	Yes	0.4" dia. Spall Crater 0.75" dia NOT punctured
O-95	CBB	395.4	0.5795	14,300	-	1 layer Al screen 0.028" 16 mesh	1.0	0.625	9.173	4[illegible] x 0.[illegible]	-		Yes	No	Hole tapered 0.5" to 0.4" dia

* Continuation of Table I given in Progress Report No. 2

** Note that the velocity limits for the reliability code given in Report No. 2 have been modified in this report

(Continuation of Table I Report No. 2 - Aluminum Steel Projectiles)

Table I. Summary of Impact Data* (Continued)

VEHICLE HULL PLATE (TARGET)

AL HT ft^{-2}	HOLE DIA. BUMPER (Inches)	SPRAY CONE DIA. (Inches)	PRINCIPAL CONE DIA. (Inches)	PENETRATED (DEPTH) (Inches)	CRACKED	BULGE ON BACK HEIGHT IN INCHES	GENERAL REMARKS AND THOSE PERTAINING TO THE VEHICLE HULL
4	0.5 x 0.55	-	-	No	Yes	.15"	8 Craters
4	0.35 x 0.4	1.5	-	No	No	-	3 Craters
4	0.3 x 0.43	1.0	-	No	No	-	7 Craters
4	-	-	-	No	No	-	Premature pellet breakup
4	0.25 x 0.4	1.5	0.5	Yes	-	-	0.45" dia. hole in plate
4	0.52 x 0.56	1.5	-	No	No	No	Edgegrain Fiberglas, Spacecraft Corp., 10 craters
4	0.3 x 0.4	1 x 1.5	0.4 x 0.6	Yes	-	-	[illegible] ft^3, Spacecraft Corp.
4	0.48	2.5	-	No	No	No	Few minor nicks on vehicle hull plate
4	0.35 x 0.53	2 x 3	-	No	No	No	Com'l. fiberglas insulating board
4	0.17 x 0.4	1.25 x 1.5	0.45 x 0.52	Yes	-	-	Com'l. fiberglas insulating board
[illegible]	0.4 x 0.43	1.4 x 2	-	Yes	-	-	3 holes 2 craters
2	0.3	-	-	Yes	-	-	
3	-	-	-	No (0.44")	No	.05"	Crater Dia. 0.75" lip .12"
5	0.45 x 0.5	0.9	-	No (0.38")	Yes	.15"	Crater 0.9" x 0.8" dia
5	0.45 x 0.5	1.1	-	No (0.38")	No	.05"	Crater 0.7" dia
9	0.31 x 0.4	2.25	1.0	No (0.38")	No	0.1"	Crater dia. 1.0"
7	0.35 x 0.38	3.0	0.5 x 0.7	Yes	-	-	0.50 dia. hole
7	0.45 x 0.5	5	0.3 x 1.2"	Yes	-	-	2 perforations of plate 0.1" x 0.2" & 0.15" dia
7	-	-	-	No (0.48")	No	.04"	0.4" dia. 0.08" lip
62	0.35	0.8	0.55	No	No	Slight	
42	0.3 x 0.35	1.2	-	No	No	Slight	Good distribution of fragments
42	0.13 x 0.28	-	-	Yes	-	-	0.45" dia. hole in plate
8	0.2 x 0.25	-	0.45	Yes	-	-	0.45" dia. hole in plate
5	0.3	-	0.4	Yes	-	-	0.4" dia. hole in plate
56	0.25	1.25 x 2.50	0.7 x 1.75	Yes	-	-	0.3" x 0.4" hole in plate

Absorbers, Steel and Copper Projectiles)

ROUND NO	REL CODE	PROJECTILE MATERIAL	WT PROJECTILE	VELOCITY Ft. Sec^{-1}	MOMENTUM Ft. Lbs - Inch^{-2} Sec^{-1}	BUMPER MATERIAL	BUMPER THICKNESS	CORE MATERIAL	SPACING (Inches)
N-132	AAC	4130-Steel	0.5750	16,200	419	Al	0.063	Min-K 1300	1.0
N-138	CAC	"	0.5680	18,900	-	Al	0.063	Potassium Titanate	1.0
N-121	-	"	0.5718	-	-	Al	0.063	Min-K 2000	1.5
O-93	CCB	"	0.5760	15,200	-	Al	0.063	Potassium Titanate	1.5
N-119	CAB	"	0.5710	12,500	-	Al	0.063	EG Fiberglas	1.5
N-120	AAB	"	0.5714	12,500	321	Al	0.063	EG Fiberglas	1.5
N-142	CAC	"	0.5762	16,200	-	Al	0.063	EGF 13	1.7
O-92	AAB	"	0.5744	14,700	380	Al	0.063	Potassium Titanate	3.0
O-67	BCB	"	0.5838	13,200	-	Al	0.063	Fiberglas	3.0
O-68	BAC	"	0.5838	17,200	-	Al	0.063	Fiberglas	3.0
N-145	AAA	"	0.5723	10,200	263	Al	0.063	Min-K 1300	3.0
D-159	ABA	"	0.5726	10,900	-	Al	0.032	Min-K 1300	2.0
D-150	-	Copper	0.6819	14,000	-	None	-	-	-
D-152	ABB	"	0.6355	13,200	378	Al	0.090	None	0.25
D-147	ABB	"	0.6593	15,200	451	Al	0.090	None	0.50
D-148	CBA	"	0.6603	10,400	-	Al	0.090	None	1.5
D-146	AAA	"	0.6706	10,800	327	Al	0.090	None	3.0
D-151	ABB	"	0.6330	12,600	359	Al	0.090	None	4.0
N-116	A	4130-Steel	0.21	11,400	-	None	-	-	-
N-122	ACB	"	0.2135	14,000	238	Al	0.032	None	0.25
N-123	ABB	"	0.2143	14,800	255	Al	0.032	None	1.25
N-124	BAB	"	0.2143	13,600	-	Al	0.032	None	0.75
N-125	CBB	"	0.2123	12,500	-	Al	0.032	None	2.25
N-127	CBB	"	0.2125	13,000	-	Al	0.032	None	6.0
N-131	CBB	"	0.2150	14,700	-	Al	0.032	None	3

* Continuation of Table I given in Progress Report No. 2.

** Note that the velocity limits for the reliability code given in Report No. 2 have been modified in this report.

Table II. Definition of Symbols Used in the Figures to Describe the Projectile Impact Conditions

ORIENTATION	INTEGRITY	IMPACT VELOCITY*
A. Projectile struck bumper nearly flat.	A. No projectile fragmentation prior to contact with the bumper.	A. Velocity less than 12,000 ft/sec
B. Projectile struck bumper on edge.	B. Very little premature fragmentation.	B. Velocity between 12,000 and 16,000 ft/sec
C. Impact angle not indicated.	C. Moderate premature fragmentation.	C. Velocity between 16,000 and 20,000 ft/sec
		D. Velocity between 20,000 and 25,000 ft/sec
		E. Velocity between 25,000 and 30,000 ft/sec

* Note that the symbols designating the velocity limits for the reliability code given in Report No. 2 have been modified (by direction) in this Report.

III. INVESTIGATION OF BUMPER EFFECTIVENESS

A. Solid Metal Bumper

A discussion of the preliminary high velocity impact data obtained with the 0.57-gram steel projectile and the 0.090- and 0.063-inch aluminum bumpers were presented in Progress Report No. 2. The importance of bumper spacing on total weight reduction, damage to the bumper (back-splash and projectile fragmentation), and vehicle hull damage dependence on momentum transfer per unit impact area, were presented phenomenologically. The preliminary data have now been verified and a reliable curve can be drawn through the experimental points.

Note that in a number of instances, with copper projectiles or with glass bumpers, experiments, which did not result in the complete penetration or cracking of the test panels, were not repeated with a reduced spacing. Experience has shown that whenever a pronounced bulge appears on the rear surface of the test panel, a small reduction in spacing will result in complete penetration and/or cracking.

1. Aluminum Bumper, Type 6061-T6, 0.125-Inch Thick

Four 0.125-inch aluminum bumpers with a spacing from 0.5- to 2.25-inches have been subjected to impact from the 0.57-gram steel projectile. The data, although incomplete, are in concordance (Figure 1) with the reference curve (see Figure 9) derived from all the impact data produced in this program. The reference curve represents the change in total weight (fixed bumper thickness plus variable vehicle hull) per area with distance of separation between the bumper and vehicle hull. All experimental points are coded for easy reference. For example, a description of the impact conditions are given in Table II for the experiment (Round No.) designated 0-80 CAB, etc., in Figure 1.

2. Aluminum Bumper, Type 6061-T6, 0.090-Inch Thick

The experimental impact data for 0.090-inch thick aluminum bumpers subjected to impact from the 0.57-gram steel projectile were given in Report No. 2. Results from four additional experiments (0-64, 0-65, 0-88, and 0-90) are in agreement with those previously presented and all data pertaining to 0.090-inch bumpers are summarized in Figure 2.

3. Aluminum Bumper, Type 6061-T6, 0.063-Inch Thick

The experimental impact data for 0.063-inch thick aluminum bumpers subjected to impact from the 0.57-gram projectile were given in Report No. 2. Results from four additional experiments (0-66, 0-82, 0-86, and 0-87) are concordant with those previously presented and all data pertaining to 0.063-inch bumpers are summarized in Figure 3.

4. Aluminum Bumper, Type 6061-T6, 0.032-Inch Thick (0.57-Gram Steel Projectile)

The experimental impact data for 0.032-inch aluminum bumpers subjected to impact from the 0.57-gram steel projectile are summarized in Figure 4. Twelve experiments were made with test panels that weighed from 11.03- to 5.74-lb/ft^2 and with a spacing from 0.25- to 4.0-inches.

Projectile orientation at the time of impact with the bumper is very critical. This orientation manifests itself in the fact that any selected bumper-vehicle hull system of fixed spacing and total weight per unit area will perform as designed when the flat face of the projectile strikes the bumper, but, will be penetrated when the edge of the projectile strikes the bumper. The total momentum for the projectile will be identical in all cases and will not depend on whether the projectile strikes the bumper flat or on edge. However, the momentum per impact area will be considerably greater when the edge of the projectile strikes the bumper; consequently, projectile fragmentation will be less and damage to the main hull of the vehicle will be greater.

Due to the sensitivity of the 0.032-inch bumper system to projectile orientation, a series of experiments were made with each test panel combination in order to obtain valid results. A projectile striking an edge which failed to completely penetrate the hull or a projectile striking flat which did completely penetrate the hull would justify a change in spacing.

The open squares in Figure 4 indicate the total weight and spacing used while the closed and open circles indicate the extent of the test panel damage. This method of reporting the data was necessary since the same test panel, depending on projectile orientation, may or may not be penetrated.

5. Aluminum Bumper, Type 6061-T6, 0.090-Inch Thick; Copper Projectile

Six test panels with 0.090-inch aluminum (Type 6061-T6) bumpers were subjected to impact with explosively accelerated copper projectiles* that were 1/4-inch in diameter by 3/32-inch thick and weighed** 0.68-gram. The data, in circles, are summarized in Figure 5 and can be compared with the data (solid line) obtained with the impact of a steel projectile on the 0.090-inch thick aluminum bumper (Figure 2). The excellent concordance between the two sets of data is obvious.

---

* The copper and 4130 steel projectiles are of identical geometry and have a mass of 0.68- and 0.57-gram, respectively. The electrolytic copper is 99.9 percent pure with the specification of QQC-502.

** Consult Table I for exact weights.

The craters produced in aluminum (6061-T6) by the copper and steel projectiles of identical size and shape but with a slightly different mass (the copper was 18.5 percent heavier than steel) can be compared from the data given in Table III and Figure 6. The non-hemispherical, somewhat cylindrical* crater produced by the steel projectile was 0.625-inch in diameter and 0.719-inch deep; however, the copper projectile produced a rather shallow crater that was nearly hemispherical* (0.75-inch diameter and 0.44-inch deep). Copper, by virtue of its low melting point and greater plasticity than steel, behaved as a semi-viscous fluid during penetration, thus developing the essentially semi-hemispherical crater which is normal for this penetration mechanism. At higher impact velocities, steel would be expected to behave similarly.

B. Glass Bumpers

Four test panels with 0.094-inch plate glass bumpers were subjected to impact with explosively accelerated steel projectiles that weighed 0.57-gram. The data, in squares, are summarized in Figure 5 and can be compared with the data (solid line) obtained with the impact of a steel projectile on the 0.090-inch thick aluminum bumper (Figure 2). The glass bumper completely fragmented on impact making it impossible to determine the projectile orientation and integrity at the instant of impact. This necessitated coding of the glass bumpers as B, C, or D. The excellent concordance between the two sets of data is obvious.

The extent of damage inflicted on a main vehicle hull that was protected (Round No. 0-60) with the 0.094-inch thick plate glass bumper spaced 1.5-inches from the hull is shown in Figure 7. This brittle and amorphous bumper material provided sufficient time and resistance to completely fragment the steel projectile traveling at 17,500 ft/sec. The crater was irregular and the area surrounding the crater was heavily pitted. It appears that the pits were produced from fragments of glass, but metallographic and spectroscopic study** will be required for verification.

C. Wire Screen Bumpers

Sixteen-mesh, 0.028-inch aluminum screen was used as a bumper in two experiments with a 1.0-inch space between the bumper and main hull of the vehicle. The bumper in experiment 0-94 was composed of two layers of screen which were pressed together. Impact from the 0.58-gram steel projectile traveling at 15,200 ft/sec produced 0.48-inch and 0.7-inch diameter holes in the first and second screens, respectively. The aluminum (6061-T6) vehicle hull was not penetrated, but a 0.4-inch circle of material was spalled from

---

* Note that the crater is not amenable to precise measurement due to the irregularities in the crater wall, lip, etc.

** These analytical studies are in progress and the results will be presented in the final report.

Table III. Comparison of Craters in Aluminum Produced with a Copper and Steel Projectile

ROUND NO.	PROJECTILE				VEHICLE HULL		CRATER DIMENSIONS* IN VEHICLE HULL (INCHES)			BULGE ON BACK OF VEHICLE HULL	
	MATL.	SIZE	MASS, GRAMS	VELOCITY, FT/SEC	MATL.	THICKNESS, INCHES	DIA.	DEPTH	LIP	DIA.	HEIGHT
J-2	Steel	1/4-inch Diameter 3/32-inch Thick	0.5742	13,500	Aluminum (6061-T6)	0.875	0.625	0.719	0.08	0.75	0.1
D-150	Copper	1/4-inch Diameter 3/32-inch Thick	0.6819	14,000	Aluminum (6061-T6)	0.875	0.75	0.44	0.12	1.00	0.08

* Note that the crater is not amenable to precise measurement due to the irregularities in the crater wall, lip, etc.

the back surface of the plate. The bumper in experiment 0-95 was composed of one layer of screen. The steel projectile, traveling at 14,300 ft/sec, produced a 0.48-inch by 0.50-inch hole in the screen. The main hull was penetrated and produced a 0.8-inch diameter shear plug which tapered to 0.4-inch.

The mesh of the wire screen was smaller than the projectile and permitted the steel projectile to partially fragment on impact. It should be noted that the screen had numerous impact holes, but these were produced by the spray of material splashed back from the 0.625-inch thick aluminum plate. This information was determined from the direction that the broken wires surrounding the hole were bent.

IV. PRINCIPLES OF METEOROID PROTECTION

The influence of material strength in semi-infinite targets is of prime importance in the low impact velocity or unbroken projectile region, but is greatly diminished at the impact velocity* of approximately 4,000 ft/sec. Impacts at this velocity are in the transition or broken projectile zone, which immediately precedes the fluid impact region (Figure 8). With a further increase in impact velocity, the effect of target strength continues to lessen. At approximately 10,000 ft/sec, the penetration in soft copper is only 12 percent greater than in hard copper. Impact at this velocity is well into the fluid impact regime, and extrapolation of the observed data indicates that penetration would be affected very little by target strength at velocities of the order of approximately 20,000 ft/sec.

A single thick plate of material cannot be considered for use in the construction and protection of a space vehicle since the vehicle would be too heavy to move from the earth's atmosphere. In addition, a single thick plate does not furnish the maximum protection for its thickness and weight per unit area. This paradox can be attributed to the propagation of shock waves through materials and to the reflection of shock waves at free surfaces which may lead to spallation. Material spalled from the inside surface can have moderately high velocity and can also cause extensive damage to the interior of a vehicle.

An energy exchange occurs when a high velocity projectile strikes any target material. The projectile will fracture or deform and mush-out as a fluid as the target material impedes the forward motion of the projectile. The fluid projectile tends to turn itself inside out which increases the diameter and results in the eruption and dispersion of some of the particles in the direction of the incident projectile. The target material, when subjected to the impact from the high velocity projectile, will behave as a fluid with almost zero shear strength.

Two cases must be considered.

A. Case I The Relatively Thin** Single Plate

Projectile impact*** at about 20,000 ft/sec on a relatively thin** single target plate will lead initially to projectile dispersion and/or fragmentation and initially the target will behave similar to a fluid (Point A, Figure 8). A large amount of energy is transferred from the projectile to the target, and therefore, the target material must be displaced under

---

* The velocity at which this transition occurs depends on the material comprising both the target and projectile.

** "Relatively thin plate" in contrast to a semi-infinite plate, refers to the minimum thickness that cannot be punctured by a given particle.

*** Projectile impact will be considered normal to the target surface.

the directed hydrodynamic forces. With the relatively thick plate or mass of material impeding this fluid motion, the displaced fluid material is forced to move from the impacted free surface since the target is not penetrated. Concurrently, the projectile, and some of the disrupted target material, is still expanding and moving deeper into the target but at a slower velocity than the incident projectile; i.e., the advancing particles of the projectile and target have a steadily decreasing velocity corresponding to points A, B_1, B_3, C_1, and O of Figure 8. At any particular instant, the target material will resist the forward motion of the incident particles. Since the forward motion or particle velocity is steadily decreasing with time, the target material is forced to behave first as a fluid (A to B_3, Figure 8), then undergo the transition corresponding to particle velocities from B_3 to C_1, and then exert its strength properties in the particle velocity region from C_1 to zero.

These deductions are based on the fact that the diameter of the hole formed in a plate increases within limits with: 1) the thickness of the plate (see Figure 23 of Report No. 2); and/or 2) the decrease in material strength.

B. Case II The Single Meteoroid Bumper

Projectile impact at about 20,000 ft/sec on a simulated vehicle structure, composed of a meteoroid bumper and main hull, will lead to projectile dispersion and/or fragmentation. The material in the bumper will behave as a fluid (Point A, Figure 8). The time for energy exchange between the projectile and bumper plate is limited since the bumper plate is thin and is readily penetrated; however, the time is sufficient to permit the projectile to lose its integrity, although the resistance presented by the bumper is insufficient to decelerate the particles from the high- to the low-velocity region. That is, penetration of the thin bumper is always in the fluid impact region and particle velocities will range from the initial impact velocity of Points A to B_3 of Figure 8. The projectile particles and shear plug material leaves the bumper and moves into the void* between the bumper and the vehicle hull. Total momentum at the instant the particles move by the rear face of the bumper is still quite high, but momentum per particle is quite low due to the large number of particles produced.

This void permits the forward moving particles to disperse** into a more or less conical spray before contacting the vehicle hull. This dispersion of the particles will result in a drastic reduction of the momentum per impact area on the vehicle hull, although the total momentum will be almost unaffected. Consequently, damage to the vehicle hull from these numerous moderately-high velocity (but very small) particles will be reduced.

---

* This void may or may not be evacuated and filled with an energy absorbing material.

** Increase the distance between the particles.

If the void is filled with an energy absorbing material, the velocity of the particles passing by the rear face of the bumper may be significantly reduced before they contact the vehicle hull. Particle velocity may be reduced from the range of Points A to B_3 down to C_1, or lower (Figure 8). In this case, the momentum per unit impact area of the forward moving particles contacting the vehicle hull is lowered by the particle dispersion as well as the reduction in impact velocity. Consequently, the material comprising the vehicle hull may be exposed to numerous particles with velocities in the range of Point C_1 or lower, and the vehicle hull should have high strength in order to absorb, without being penetrated, all the energy of the impinging low velocity particles.

It can be deduced that a void filled with energy absorbing material provides a discontinuity in the penetration-impact velocity curve of Figure 8. Due to this discontinuity, the total weight per unit area of the vehicle can be reduced. With this concept, the meteoroid bumper must have mass, with no strength requirements, while the vehicle hull must have high strength to prevent penetration from the relatively low velocity particles.

C. Summary

The effectiveness of the meteoroid bumper depends entirely on its mass; it does not need to possess strength or toughness since the impact processes are fluid. This principle permits a wide selection of materials, and bumpers of solid metal, plate glass, and wire screen have been found to be equally effective on the basis of comparable mass. Further weight reduction of the bumper system can be obtained by proper spacing.

Supporting data have been established for steel projectiles with a mass of 0.57-gram. Bumpers with a range of thickness of 0.032- to 0.125-inch provided the necessary impedance to this projectile to bring about fragmentation, thereby preventing serious damage to the vehicle hull. For a given hull thickness, the corresponding minimum bumper mass may be obtained from the established relationships between total weight and spacing. In weight conscious design, spacing should be at least two inches.

The preliminary impact data are summarized in Figure 9. Very little difference can be seen in the various bumper materials investigated with a two-inch spacing. Beyond two inches, projectile orientation, fragmentation, etc., do not permit an accurate assessment; however, the decrease in weight in the first two-inch spacing is the most significant.

Additional experiments now in progress, introducing the variation of projectile mass, absorber material, and several parametric influences, are expected to provide further verification of the established bumper concept.

V. LOW MASS PROJECTILE

An aluminum bumper, 0.032-inch thick, spaced from zero to six inches from aluminum vehicle hulls of variable mass, has been subjected to impact from the 0.21-gram, cylindrical steel projectile 0.063-inch thick and 0.188-inch in diameter. All impact data are summarized in Figure 4. It should be noted that a new fiducial point was determined (N-116) for a single thick plate requiring 8.87 lb/ft^2 to prevent penetration, spallation, or cracking as a result of impact from the 0.21-gram projectile. This can be compared to 12.43 lb/ft^2 required for the 0.57-gram projectile. These data must be considered preliminary, but several tentative statements can be made: 1) Penetration is less severe with the smaller projectile; and 2) the total weight per unit area for any given spacing between the bumper and vehicle hull appears to be proportional to the thickness of a given steel projectile. For example, the thickness of the 0.57-gram projectile is 1.5 times that of the 0.21-gram projectile and the total weight per unit area to prevent penetration from the 0.57-gram projectile is about 1.5 times greater.

VI. PRESSURIZED STRUCTURES

Space vehicles will have components pressurized with a fluid; gas and liquid fuel tanks, liquid working fluid for radiators and gas for inflatable and manned structures. Pressurized structures, especially liquid filled components, present formidable protection problems due to the difference in materials and component behavior when subjected to hypervelocity impact.

The kinetic energy of a high velocity particle is delivered to a liquid pressurized tank at an extremely high rate. Since this energy supplements the hoop tension existing in the vessel wall, failure can be expected at the point of particle impact. This has been observed and preliminary puncture (projectile velocity of approximately 17,000 ft/sec) will be followed by catastrophic ripping (Figures 10 and 11) of the vessel wall by stored energy due to the hoop tension stresses. Gas pressurized structures may behave in an entirely different manner (Figure 12). The kinetic energy is delivered to the walls at a slower rate (relative to the liquid filled tank) due to the low gas density and low speed of sound. Therefore, failure can be expected via puncture, spall and continued flight of the hypervelocity particles through the gas and out the opposite side of the tank. If, however, the crack or tear produced in the wall of the gas pressurized tank exceeds the critical crack length of the material for the wall stresses which prevail, catastrophic fracture of the tank wall may occur just as in the case of the liquid filled tank.

In addition to these obvious hazards, other perils exist which are frequently not recognized. For example, an astronaut may: 1) experience shock and/or concussion; and 2) be subjected to a flash explosion from the high velocity impact with an oxygen-rich pressurized space vehicle. Also, liquid-oxygen propellant storage tanks may explode since they will contain both liquid and gaseous oxygen.

In order to determine the extent of damage as well as to study the impact flash and explosions resulting from meteroric particle impact on oxygen-rich pressure vessels, a six-inch diameter by six-inch long cylinder was fabricated with replaceable end diaphragms. These test containers were subjected to impact with the 0.188-inch diameter by 0.063-inch thick explosively accelerated steel projectile.

A. Test Panel No. 1

The front and back diaphragms (0.025-inch thick) of the test cylinder were fabricated from the 5Al-2.5Sn titanium alloy, and the system was pressurized to 20 psi with pure gaseous oxygen. The 0.2110-gram projectile, with an impact velocity of 15,900 ft/sec, formed the 0.33-inch diameter hole and the 0.75-inch diameter oxidized and burned area in the front diaphragm (Figure 13). Impact with the titanium alloy plate fragmented the projectile but did not prevent particles from penetrating the rear diaphragm. This rear diaphragm burned rapidly in the oxygen-rich environment and produced a burned out area of about four inches in diameter. Ignition appears to have originated from at least three points.

B. Test Panel No. 2

The front and back diaphragms (0.010-inch thick) of the test cylinder were 301 extra-full-hard stainless steel and the system was pressurized to 60 psi with pure gaseous oxygen. The 0.2154-gram projectile, with an impact velocity of 13,600 ft/sec, formed the 0.25-inch diameter hole (Figure 14) in the front diaphragm. Fragmentation of the projectile was extensive as evidenced from the numerous small holes in the rear diaphragm. An explosion was initiated as a result of the impact and the rear diaphragm was ruptured, but only after it was penetrated from the forward moving fragments. Two pieces of the rear diaphragm were found.

Several additional impact tests will be made with 0.1-gram projectiles* on aluminum, stainless steel, and titanium alloy diaphragms, using liquid, gaseous, and liquid-gaseous oxygen systems. The impact phenomena will be monitored with Fastax and Dynafax high speed cameras.

Photographs of one test cylinder were obtained at the rate of 25,600 frames per second (±1000) and an exposure time of one microsecond using a Beckman & Whitley, Model 326, Dynafax camera (Figure 15). The projectile broke in at least two pieces as evidenced from the two flame jets shown in Frame 1 of Figure 15. Details of the burning cannot be followed since the entire area of the front diaphragm is obscured with the cloud of many fine particles of titanium alloy, titanium oxide(s), iron and iron oxide(s). Oxidation is quite rapid as evidenced from the progressive increase in illumination of this cloud of material.

* Projectiles weighing 0.097-gram can now be accelerated without fragmentation.

VII. ENERGY ABSORBERS

The energy absorbing or core material must have moderate compressive and shear strength, low density, directionality of mechanical properties and low ablation rates. In addition, the material must not contribute to the shock cone or to the fast moving fragments. Also, it should be capable of reducing the velocity of all particles moving toward the main hull. Thermal stability, moderate toughness, and a uniform texture are also desirable. The energy absorbing material will also serve to support, stiffen, and hold the bumper and main hull in their respective positions.

Three insulating materials (fiberglas in Figure 16, Min-K in Figure 17, and potassium titanate in Figure 18) have been subjected to preliminary impact investigation with 0.57-gram steel projectiles. All test panels were fabricated from 6061-T6 aluminum and the bumper thickness was held constant at 0.063-inch.

A 1.5-inch thick pad of fiberglas was placed in contact with the bumper and a 1.5-inch spacing was provided between the fiberglas and the main hull. Panel 0-67 defeated the projectile while panel 0-68 was completely penetrated. These results were not unexpected, since the projectile struck the bumper on edge. In the case of panel 0-67, the projectile was moderately fragmented during acceleration. This permitted the momentum per unit impact area (panel 0-67) to be reduced. Panels N-119 and N-120 were fabricated from 1.5-inch thick pads of edge-grain fiberglas with a density of 10 lb/ft^3. Panel N-120 was not penetrated since the projectile did not fragment prematurely and it struck the bumper flat. However, panel N-119 was penetrated since the projectile struck the bumper on edge.

Two test panels were fabricated with Min K-1300. Panel N-132 with a one-inch thickness prevented complete penetration, although the main vehicle hull was cracked. Panel N-145, with a three-inch thickness and weighing 0.866 lb/ft^2 less than panel N-132, was completely penetrated.

Three test panels were fabricated with a one-inch thick pad of fibrous potassium titanate. The weight of all panels was held constant at 5.93 lb/ft^2 and the total thickness of the test panel was varied from one to three inches. None of the test panels were penetrated. It should be observed that the one-inch thick panel (N-138) was struck on edge with the projectile traveling at 18,900 ft/sec.

On the basis of these preliminary data, it can be concluded that energy absorbing material placed between the bumper and the main hull of the vehicle will greatly improve the efficiency of the meteoroid protection system. For example, the total weight per unit area can be lowered from approximately 9.2 to 5.9 with the incorporation of a one-inch thick pad of fibrous potassium titanate. It should be recognized that further improvement may be forthcoming, since panel N-138 may not represent the minimum spacing for the 5.93 lb/ft^2 panel.

Two test panels were fabricated from a honeycomb-core material, which is a different type of energy absorber. Test panel I was composed of honeycomb with 0.75-inch cells*, made from 0.005-inch commercial aluminum foil placed between 0.040-inch plates of 2024-T86 Alclad. The honeycomb was bonded to the skins with Aerobond adhesive 422. This panel (Figure 19) was subjected to impact (in air) from a 0.063- by 0.19-inch, 0.2144-gram steel projectile traveling at 13,200 ft/sec. Two small fragments were broken from the projectile. The two fragments and the remainder of the projectile penetrated the two-inch thick panel as well as the 0.125-inch aluminum (6061-T6) plate placed 6.75 inches behind the test panel. The honeycomb was deformed extensively due to the explosive impact.

Test panel III was composed of honeycomb with 0.75-inch cells made with 0.005-inch commercial aluminum foil placed between 0.050-inch plates of 5-ply Conolon 506. The honeycomb was bonded to the skins with Aerobond adhesive 422. This panel (Figure 20) was subjected to impact (in air) from the 0.063- by 0.19-inch, 0.2108-gram steel projectile traveling at 16,100 ft/sec. The back skin was completely removed from the test panel as a result of the impact and the projectile fragments penetrated the 0.125-inch aluminum (6061-T6) plate placed 6.75 inches behind the test panel. The honeycomb was deformed extensively due to the explosive impact.

---

* Plastilock 620 was used for the intercellular adhesive.

VIII. PROJECTILES

A. Physical State

The physical state of the projectile apparently does not influence the penetration damage to semi-infinite plates. Penetration dependence on impact velocity of solid aluminum*, liquid** mercury and water projectiles on 1100 and 2024 aluminum is given in Figure 21. Unfortunately, the maximum liquid-impact velocity is 2624.7 ft/sec. The penetration damage in 2024 aluminum, at the impact velocity of 2231 ft/sec, is directly proportional to the projectile density; P/D values of 0.101, 0.27 and 1.38, for water, aluminum, and mercury projectiles, respectively. This analogy cannot be carried out at high velocities due to the absence of any pertinent data for liquid projectiles.

B. Glass Projectiles

Spherical glass projectiles, 0.158-inch in diameter and weighing 0.075-gram, have been accelerated with a light gas gun. Projectiles maintained their integrity during acceleration and struck the one-inch thick aluminum plate in vacuum. One projectile, traveling at 12,000 ft/sec, produced a crater that was nearly hemispherical (Figure 22); approximately 0.19-inch deep, approximately 0.32-inch in diameter, with a 0.02- to 0.05-inch lip.

---

* Presented at the Hypervelocity Impact Symposium, Denver, Colorado, 1961, by Dr. R. L. Bjork.

** "A Study of Rain Erosion Testing Methods For Supersonic Speed," D. E. Hurd and R. F. Holmes, WADC Technical Report 53-173, Part VI, January 1960.

IX. PHOTOGRAPHIC ANALYSIS OF IMPACT PHENOMENA

A. Low Speed Photographs

The caliber .30-06 projectile, with a velocity of 3030 ft/sec, penetrated the 0.125-inch and the 0.250-inch aluminum (6061-T6) plates spaced four inches apart (Figure 23). The diameter of the hole in the first and second plates are 0.3 and 0.35 inch, respectively, and can be compared to the initial projectile diameter of 0.3-inch. The grooves in the wall of the hole in the first plate correspond to the rifling on the projectile. Photographs of the impact were taken at the rate of 2886 frames per second (Figure 24). Frame No. 1 shows the bullet and shear plug fragments passing through the first plate. Frame No. 2 shows: 1) the spray of particles moving away from the front surface of the first plate at an angle of approximately 42°; and 2) the impact flash and the bullet with the shear plug fragments moving through the second plate; and 3) the lip formed on both faces of the first plate. It should be noted from Figure 23 that the second plate was struck with numerous small fragments as well as the projectile. The hole has very smooth walls and appears to have been fluid sometime during the penetration.

B. Moderate Speed Photographs

The flash resulting from the impact of the 0.55-gram, 15,800 ft/sec projectile on four spaced plates is given in Figure 25. The first-two and second-two plates were magnesium AZ-31A and aluminum 2024-T3, respectively. The luminosity that is produced is above the bright sunshine which appears as the black background. The four plates were completely penetrated. The extent of damage to each plate can be summarized as follows:

Plate 1. Two holes; 0.58- and 0.18-inch diameter.

Plate 2. Four-inch diameter of small perforations.

Plate 3. Six-inch diameter of small craters and a 1.5-inch diameter of perforations.

Plate 4. Four-inch diameter of small craters and a 2.5-inch diameter of perforations.

It can be seen that the impact flash at the surface of a plate is considerably greater in volume than at the exit side. For example, the size of the flash at the front of Plate 2 is greater than at the reverse side and the same phenomena occurs at the opposite faces of Plates 3 and 4. This can be attributed to the fact that the flash at the front of the plate is produced by the impact of many particles, and that not all particles penetrate the plate. The flash at the reverse side of the plate is produced by the particles which have penetrated the plate as well as those particles produced from the shear plug and via spallation. Some of the projectile and

ar plug particles continue on a straight line trajectory while some of the shear plug and ll material leaves the rear of the plate at an angle, which generates the luminous cone is observed.

C. High Speed Photographs

High speed photographs of the impact phenomena were taken after fixed periods ıpsed time with the Beckman & Whitley, Model 326, Dynafax camera. Two different, but ·esentative photographic sequences are shown in Figures 26 and 28.

The photographs shown in Figure 26 were taken at 26,500 frames per second 00 frames per second). The impact velocity of the 0.58-gram projectile on the test panel 9700 ft/sec. Three aluminum plates comprised this panel; the first two plates were 5-inch thick and spaced three inches apart, while Plate 3 was 0.250-inch thick and placed inch from Plate 2. The projectile maintained its integrity on acceleration, as evidenced ı the uniform impact flash (Frame 1 of Figure 26) and inspection of the front surface of irst bumper plate (Figure 27). The dimensions of the hole or shear plug varied from 4- to 27/64-inch. The ball of material (projectile plus shear plug), as seen in Frame 1 gure 26, was about 45/64-inch, which is almost twice the diameter of the hole. Thus, n be deduced that either the projectile punched a hole in the bumper that was originally ·r and there is rebound* in the bumper material as the elastic stresses in the main body ɜ bumper relax, that luminosity increases the absolute volume, or that the ball of frag- ary material is increasing its volume. This latter deduction appears to be the most ble, especially since the impact flash is spread over a 3.625-inch diameter circle re 26) and the small craters and pit-marks over a 4.5- to 4.75-inch diameter circle of ɜcond plate. These craters and pit marks are probably formed from the particles dis- d from the first plate. The main hole (15/32-inch) in the second plate was probably ɜd from particles of the original projectile, since the impact velocity (9700 ft/sec) was ›w to completely fragment and disperse the particles of the incident projectile. Material ng through the second plate impinged-on and cracked, but did not penetrate the third

The photographs shown in Figure 28 were taken at 25,800 frames per second) frames/sec). The impact velocity of the 0.57-gram projectile on the test panel was 0 ft/sec. Four aluminum plates, each 0.125-inch thick, with the spacing indicated used to form the test panel. The projectile broke into five fragments on acceleration denced from inspection of the bumper plate (Figure 28). Four of these fragments pene- the bumper, three of them very close together. These three fragments formed the (one-inch wide) cloud of material that can be seen between the bumper and Plate 2 in ɜ 1 of Figure 28. The second cloud (7/16-inch wide) of material, directly below the cloud, resulted from penetration of the bumper by the fourth projectile fragment. The

bound may account for about 10 to 20 percent.

incident particle velocity was sufficiently high to completely disrupt the integrity of the projectile particles so that the cloud of fragments was dispersed over a large area of the second plate. In fact, the momentum per unit impact area was so low that the 0.125-inch plate was bent and only three small holes were formed in the second plate. Two of these holes were barely through the second plate and produced small nicks on the surface of the third plate. The third hole in Plate 2 was produced with a fragment that formed a crater, but did not penetrate the third plate. The bottom of the crater in the third plate was pressed into the front surface of the fourth plate and produced the small indentation seen in the appropriate photograph of Figure 29. The third plate was not bent, and the depth of the punched material was 0.250-inch (0.125-inch in the plate plus the 0.125-inch in the gap between Plates 3 and 4).

APPENDIX A

PROJECTILE ORIENTATION AND FRAGMENTATION*

The cylinderical projectile will tilt or tumble during acceleration and flight to the test panel. Projectile orientation effects are diminished when: 1) the test panel is thick and only a crater is formed; or 2) if the projectile has a very high velocity when it strikes and forms a hole in a thin test panel.

Different results are observed when a steel projectile traveling at 10,000 to 20,000 ft/sec strikes a thin plate or a bumpered test panel: an edge impact produces deeper penetration and more extensive damage than a flat-face impact. When a cylindrical projectile strikes the bumper flat (see Figure 30) the hole (shear plug) formed in the bumper is round and the particles of projectile as well as the fragments from the shear plug produce a uniform pattern of small craters in the main vehicle hull. The diameter of this pattern of small craters depends, among other things, on the distance between the bumper and the vehicle hull. This distance provides time for the particles to increase their distance from each other; i.e., a circular cone of material is formed with the cone apex at the rear face of the bumper and the cone base at the front face of the vehicle hull. The further the two plates are apart, the greater the area of the cone base; consequently, the uniformly distributed particles impact over a larger area on the vehicle hull. This decrease in impact momentum per unit area of vehicle hull manifests itself by reducing the damage to the hull.

There are significant differences in the impact pattern(s) formed when the edge rather than the flat face of the projectile strikes the bumper. An edge impact will produce an elliptical hole in the bumper as well as an elliptical pattern of small craters in the vehicle hull. However, the major axis of the hole in the bumper does not coincide with the major axis of the crater pattern: i.e., the major dimension of the hole in the bumper and the crater pattern are rotated 90 degrees as seen in Figure 31. In addition, the particle distribution is not uniform, is concentrated in the central region, and results in greater penetration than observed with a flat face impact.

Impact patterns on vehicle hulls protected by a bumper show craters which could only be produced by discrete particles. In a preliminary attempt to ascertain the fate of the steel projectile and the aluminum shear plug, an 0.57-gram projectile was fired through an 0.090-inch bumper. A block of paraffin was placed behind the aluminum plate. Three magnetic fragments were recovered (0.0341-, 0.0253- and 0.0113-gram) as well as a quantity of gray magnetic paraffin. Microscopic examination of these three particles showed that melting occurred on one surface with jagged fracture on the opposite surface. These fragments evidently were from the perimeter of the projectile.

---

* See Section III-A-4.

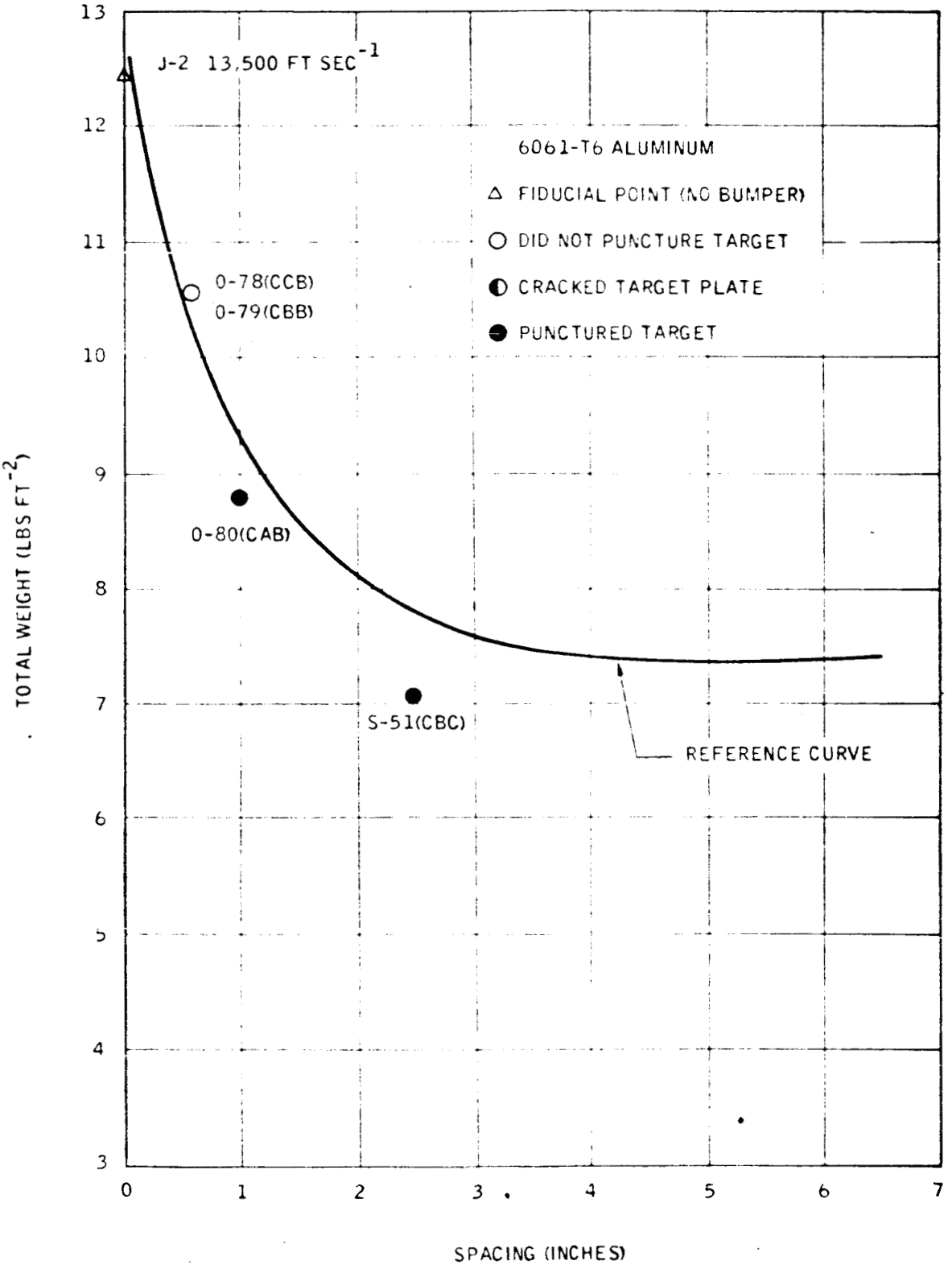

Figure 1. Mass and Spacing to Prevent Penetration (0.125-Inch Bumper)

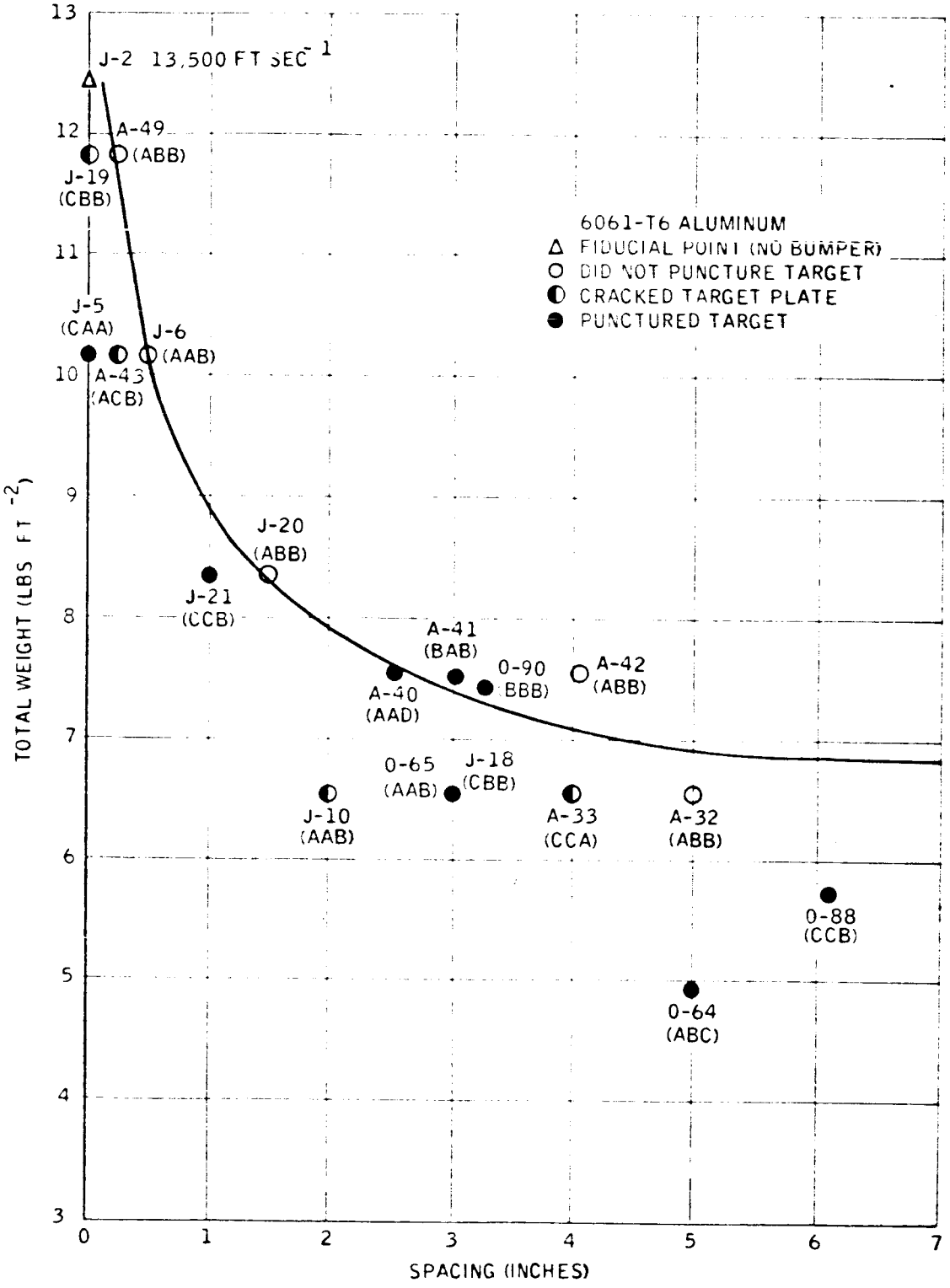

Figure 2. Mass and Spacing to Prevent Penetration (0.090-Inch Bumper)

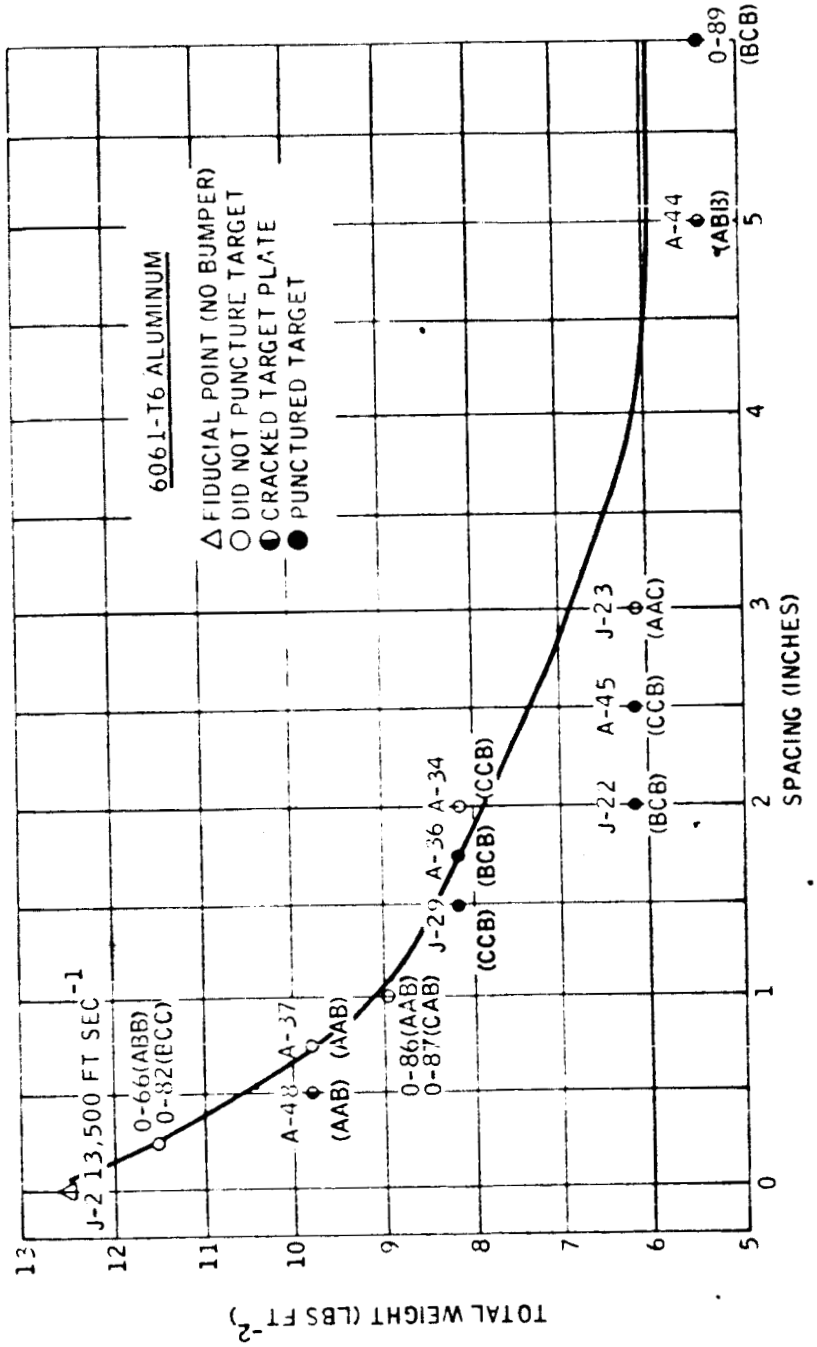

Figure 3. Mass and Spacing to Prevent Penetration (0.063-Inch Bumper)

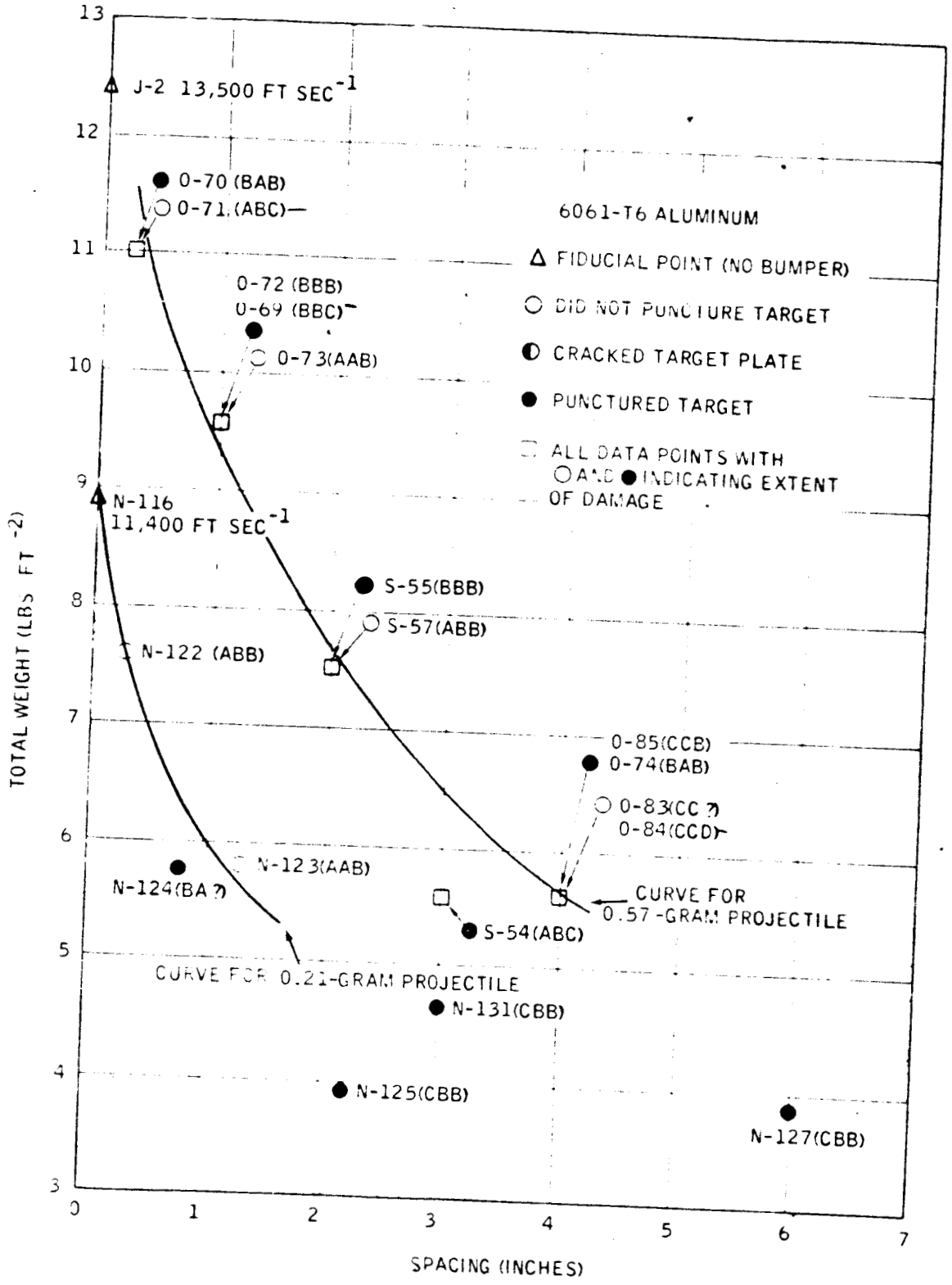

Figure 4. Mass and Spacing to Prevent Penetration (0.032-Inch Bumper)

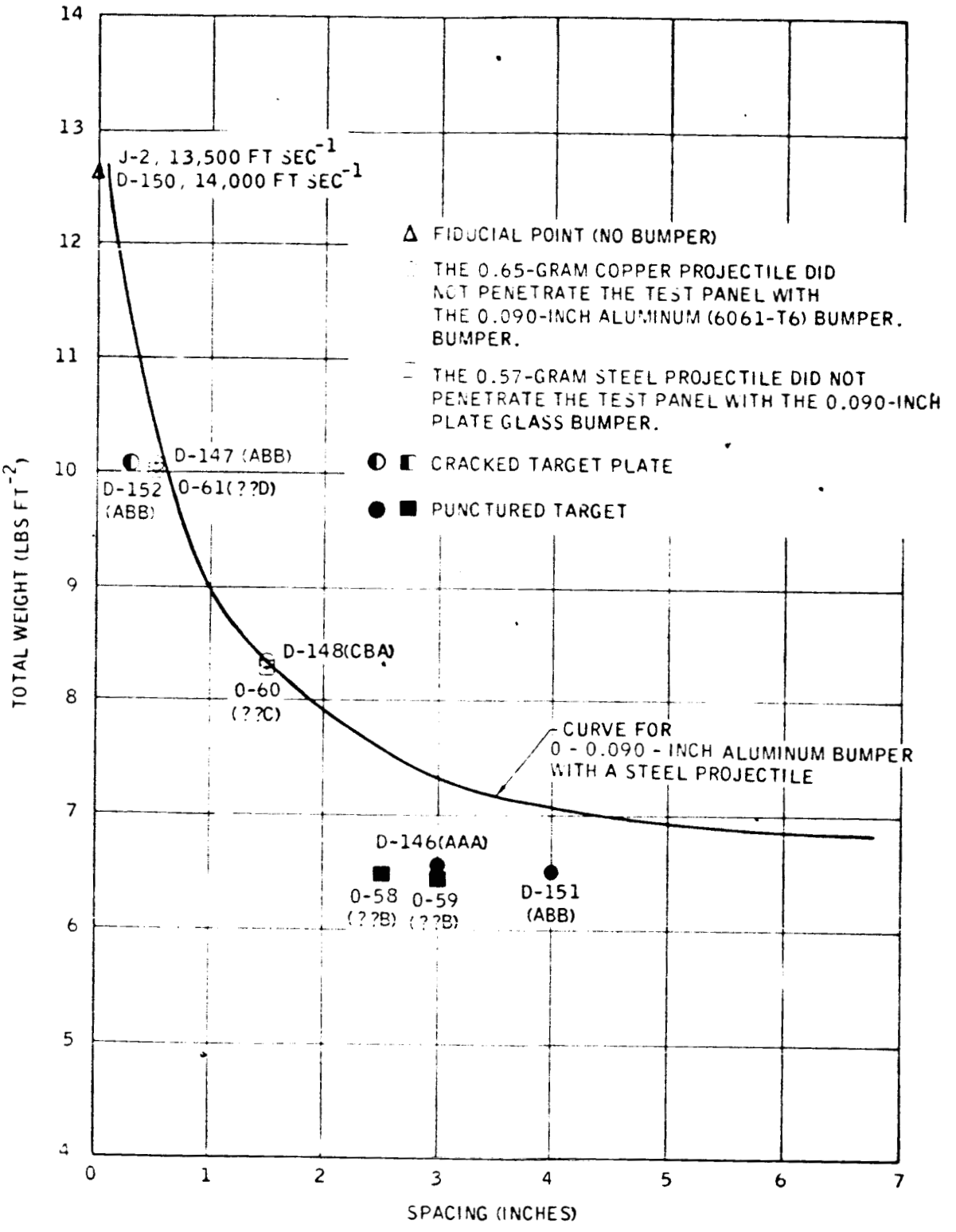

Figure 5. Mass and Spacing to Prevent Penetration (Aluminum and Plate Glass Bumpers)

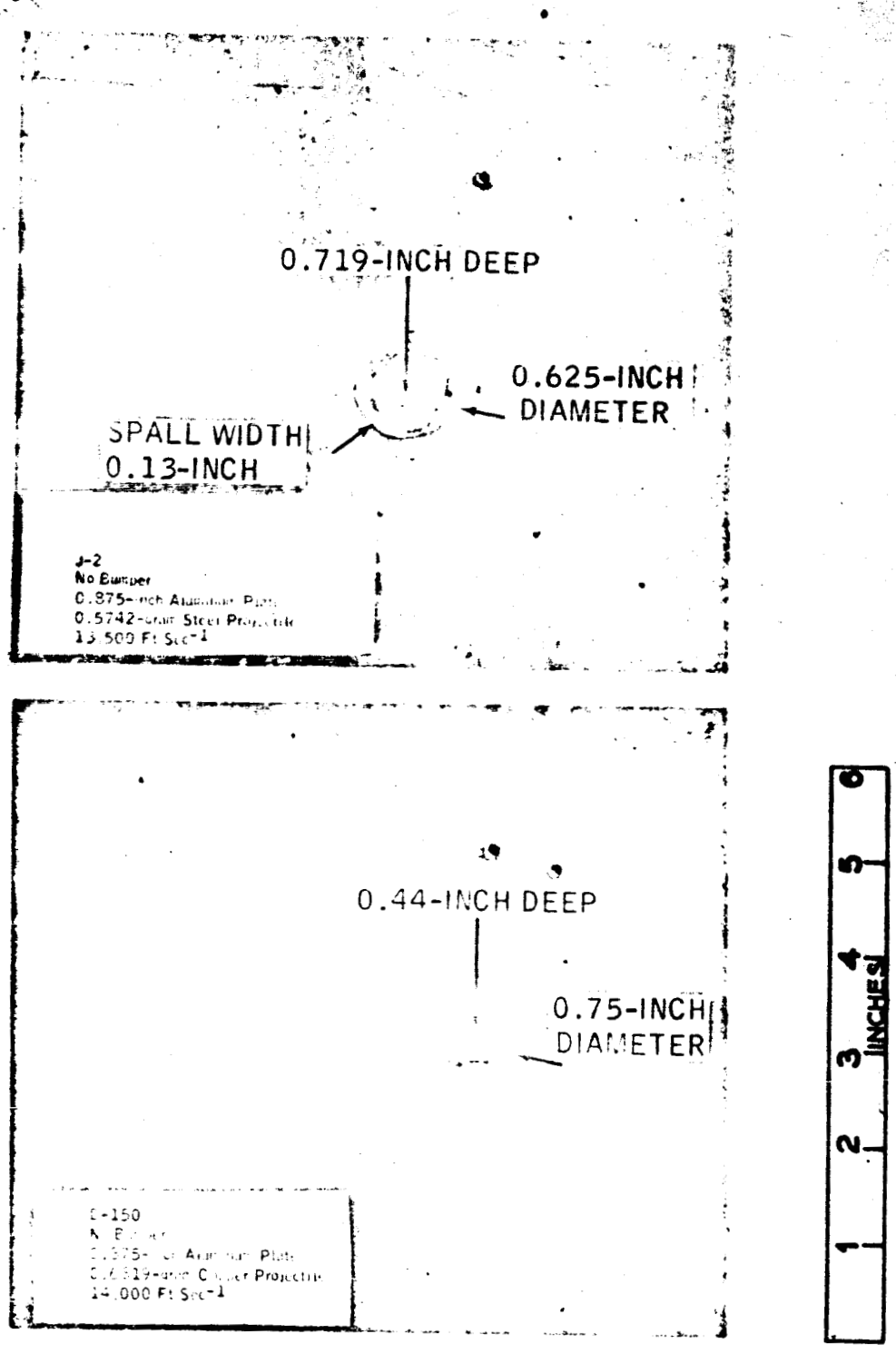

Figure 6. Craters Produced in Aluminum with Copper and Steel Projectiles

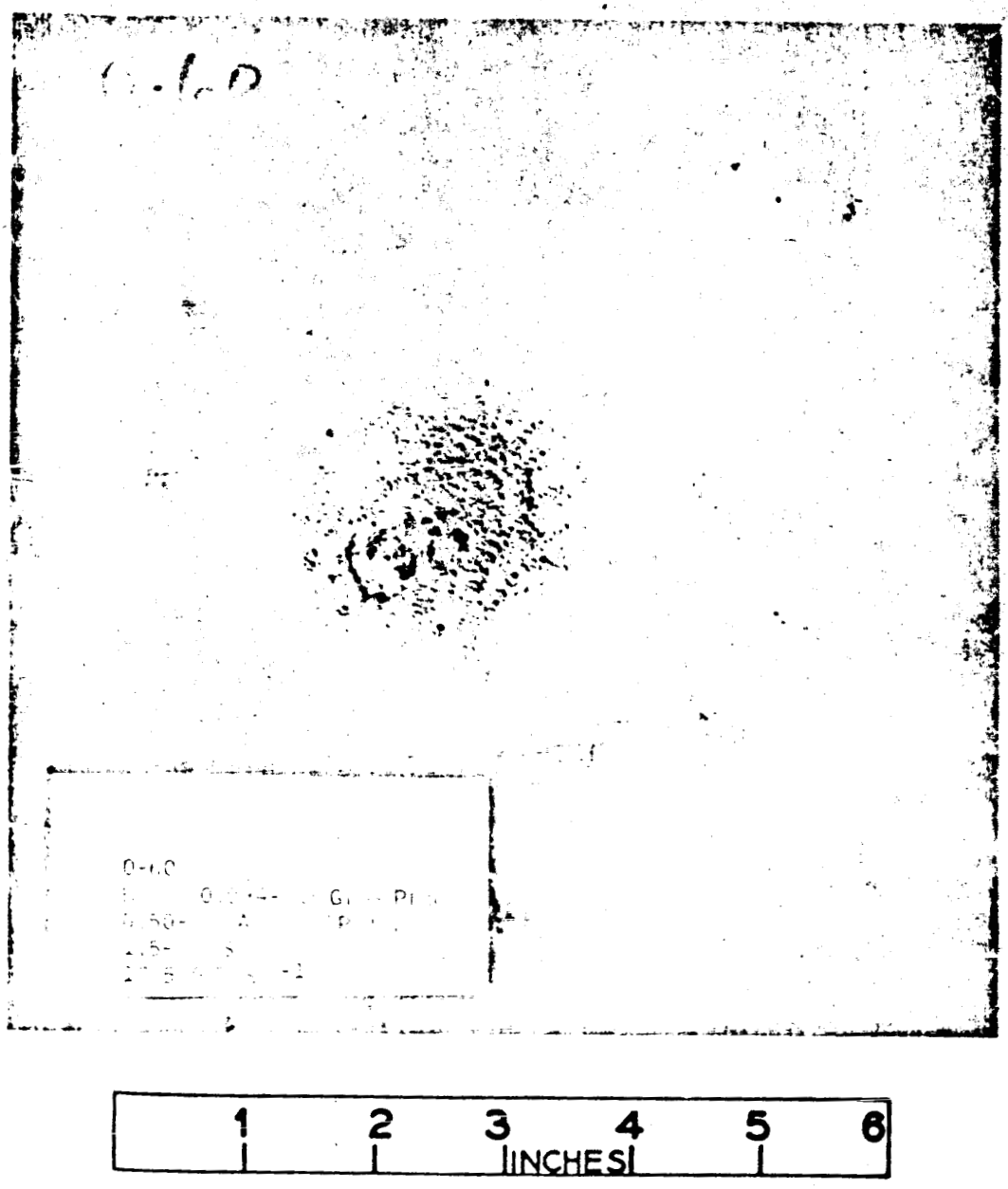

Figure 7. Vehicle Hull Protected with the 0.094-Inch Plate Glass Bumper

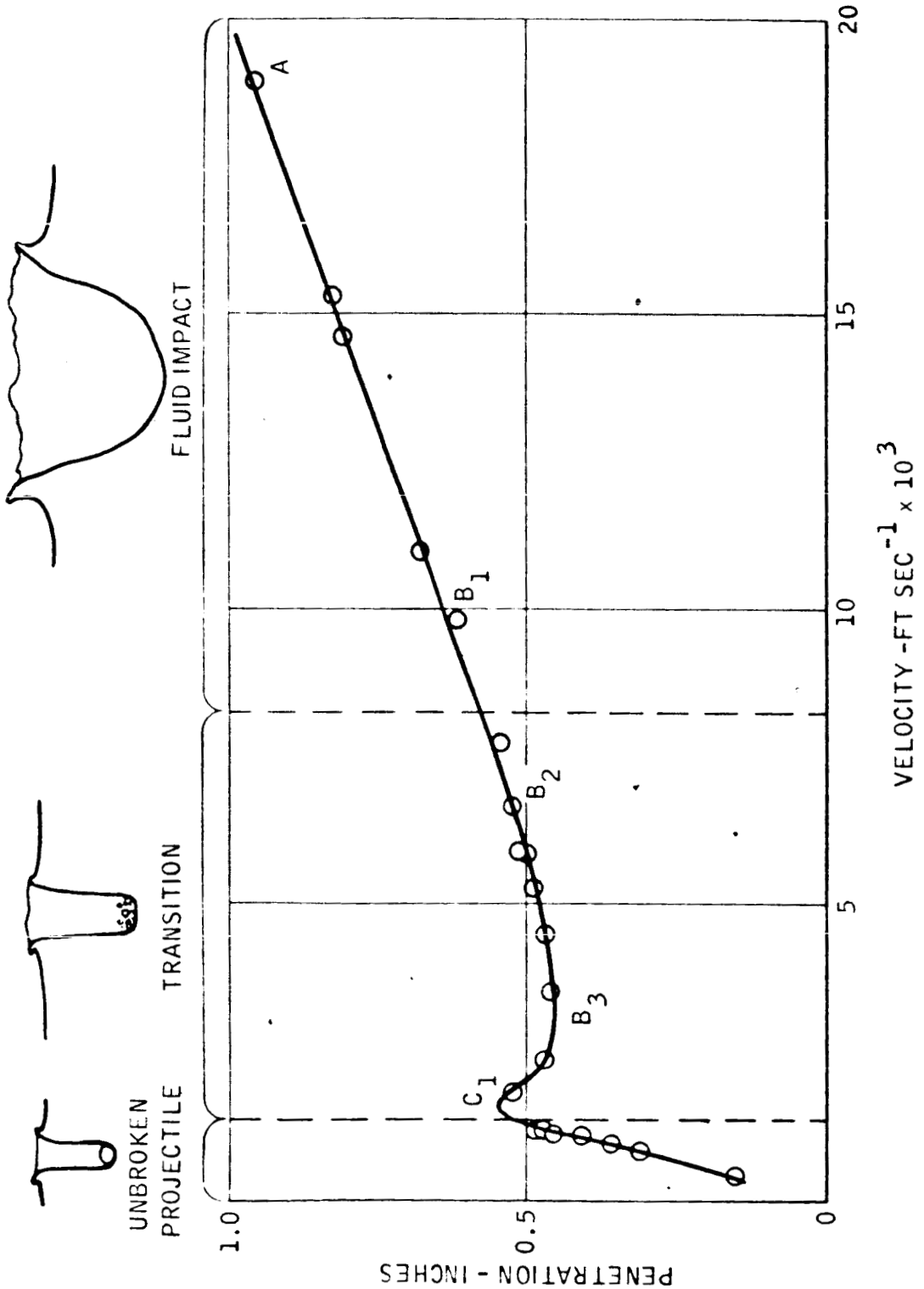

Figure 8. The Effect of Velocity on Penetration

Tank Pressurized With Water

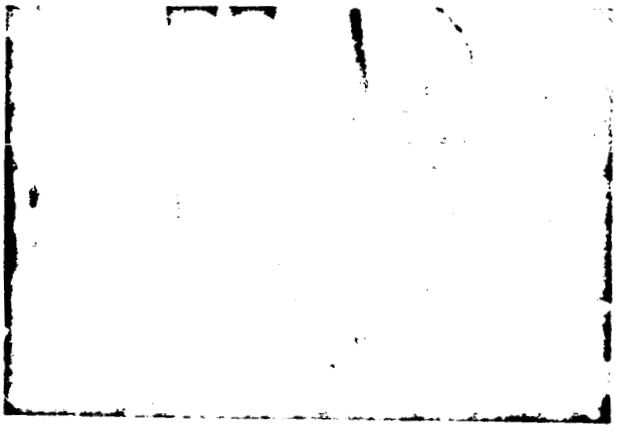

Instant Of Impact

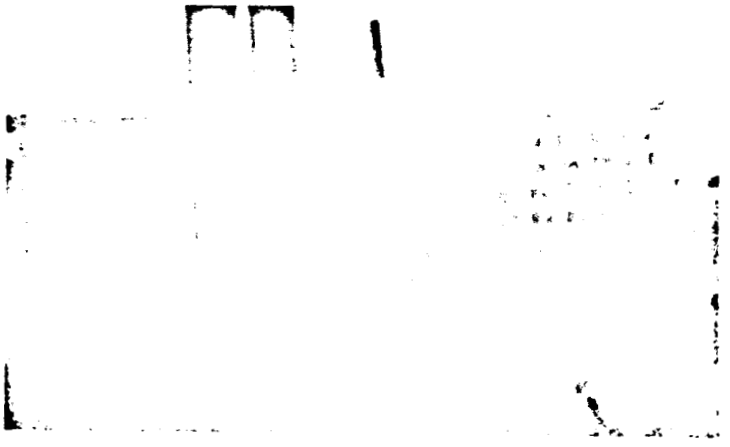

The Pellet Did Not Pass Through The Tank,
But The Tank Ruptured.

Figure 10. Liquid Pressurized Tank During Impact

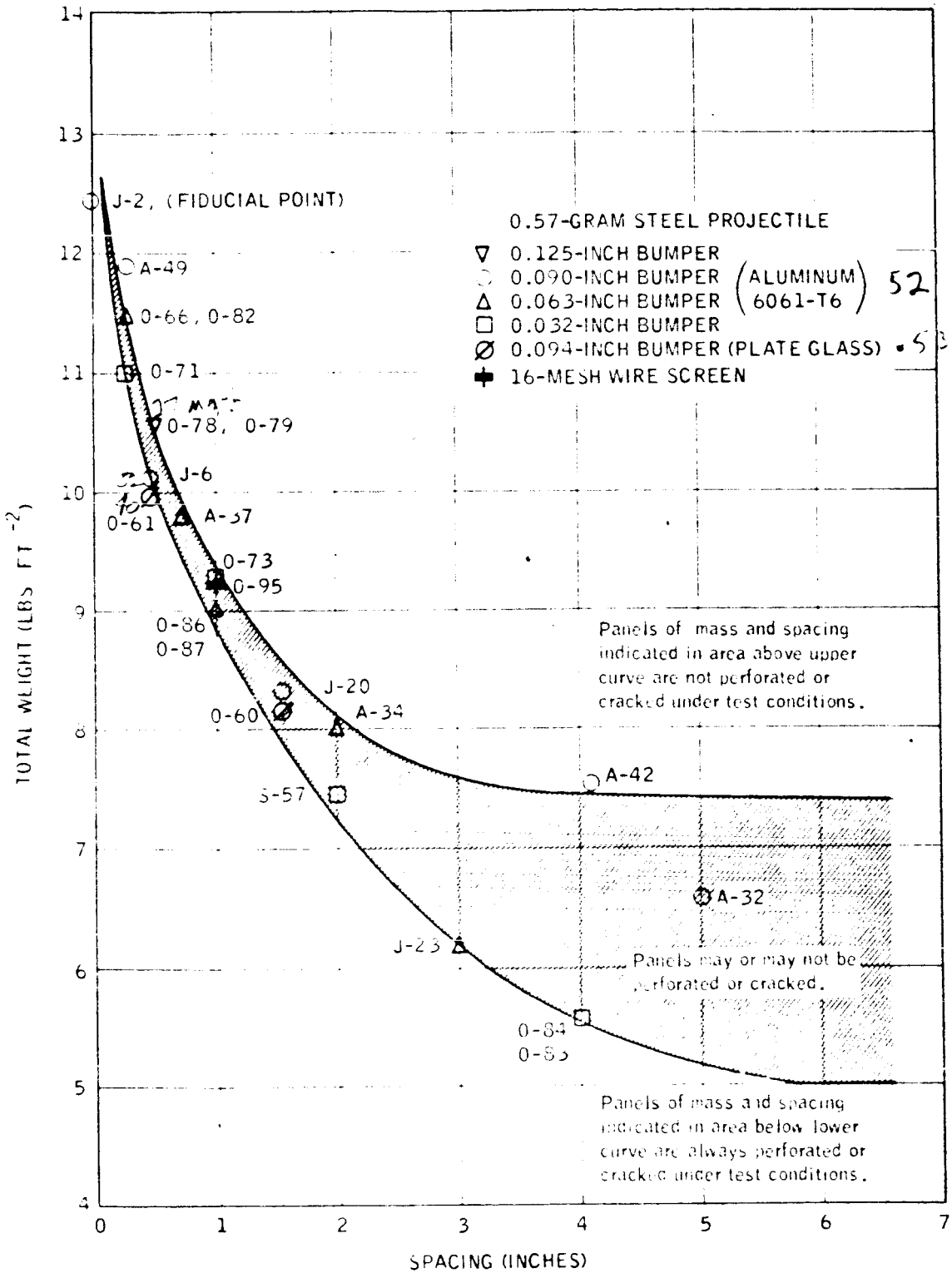

Figure 9. Mass and Spacing to Prevent Penetration (0.032- to 0.125-Inch Bumper)

DAMAGE TO LIQUID PRESSURIZED TANK

Figure 11. Liquid Pressurized Tank After Impact

Tank Pressurized With Air At Instant Of Impact

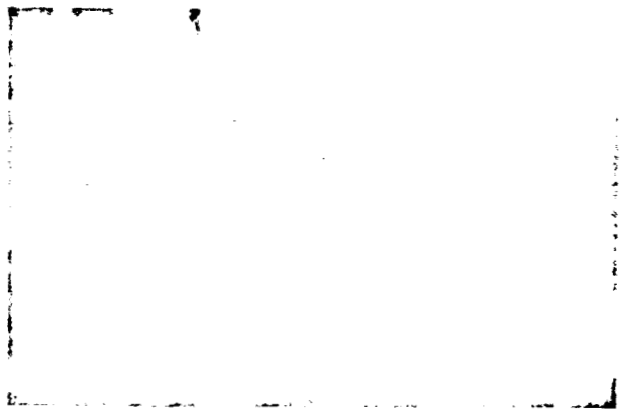

Pellet Passed Through The Tank

Figure 12. Gas Pressurized Tank During Impact

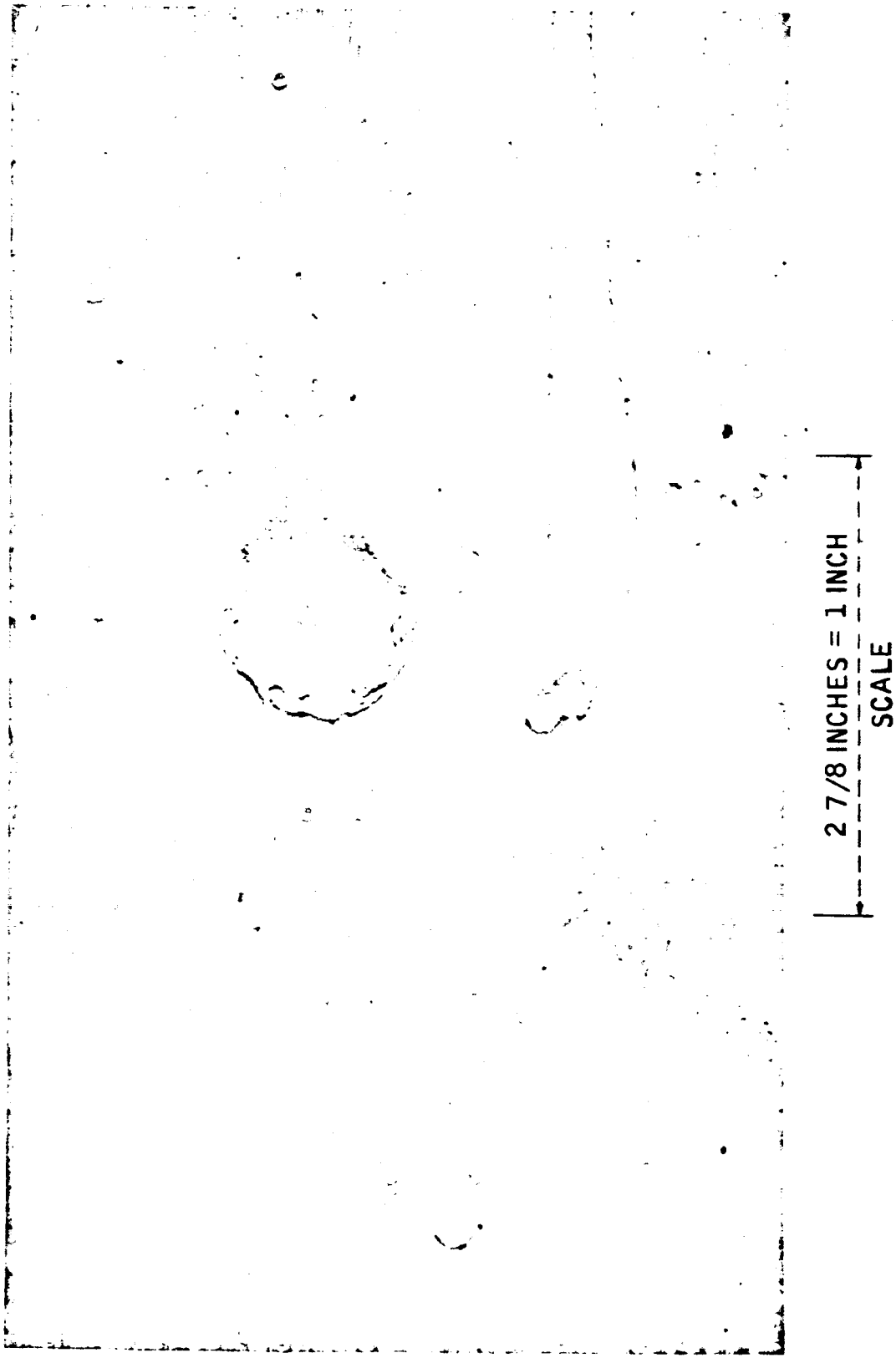

Figure 22. Glass Projectile Damage to an Aluminum Panel

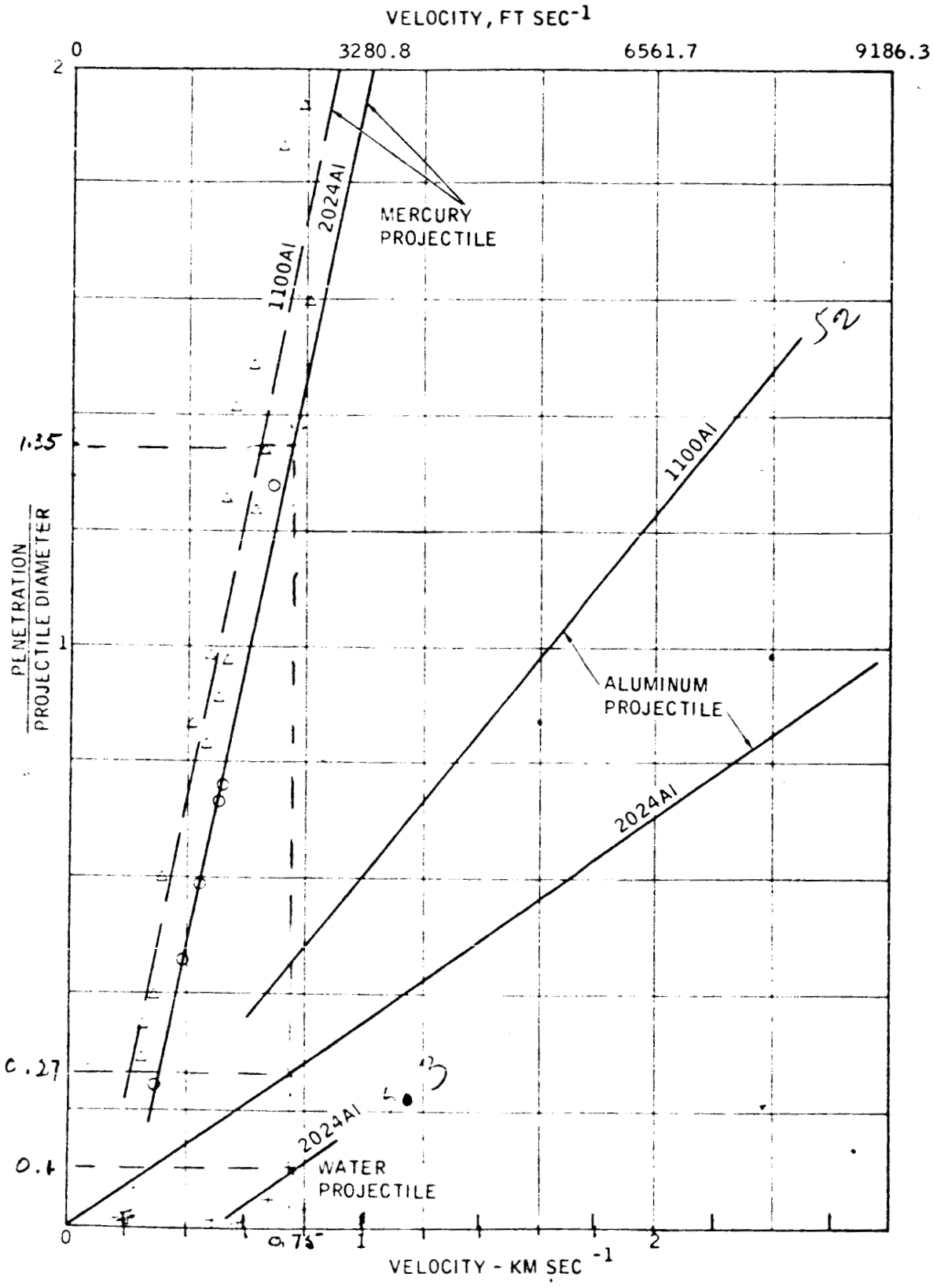

Figure 21. Penetration Dependence on Impact Velocity of Solid and Liquid Projectiles

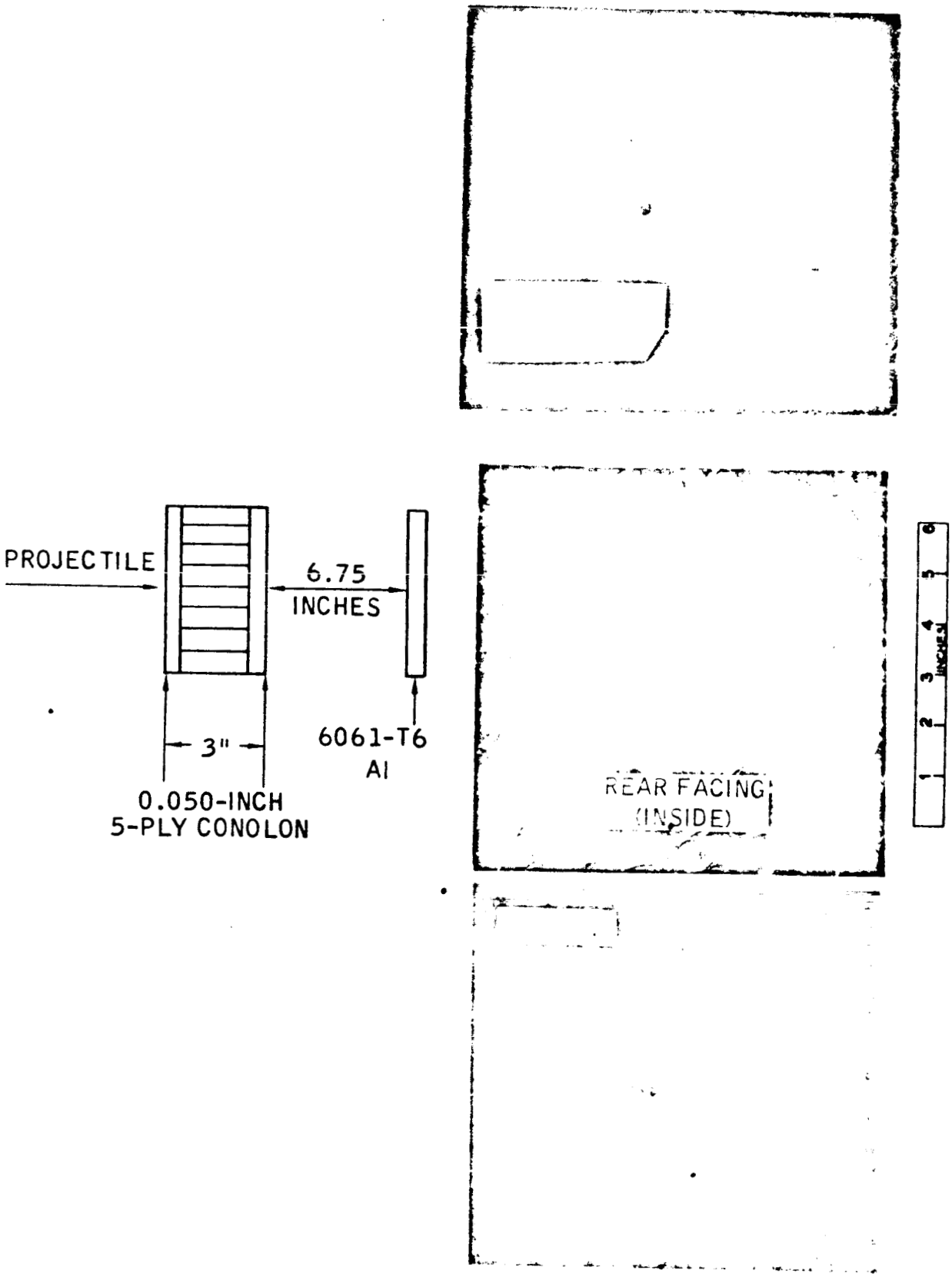

Figure 20. Honeycomb Panel No. 2
(Impact Delaminated Rear Facing from Core)

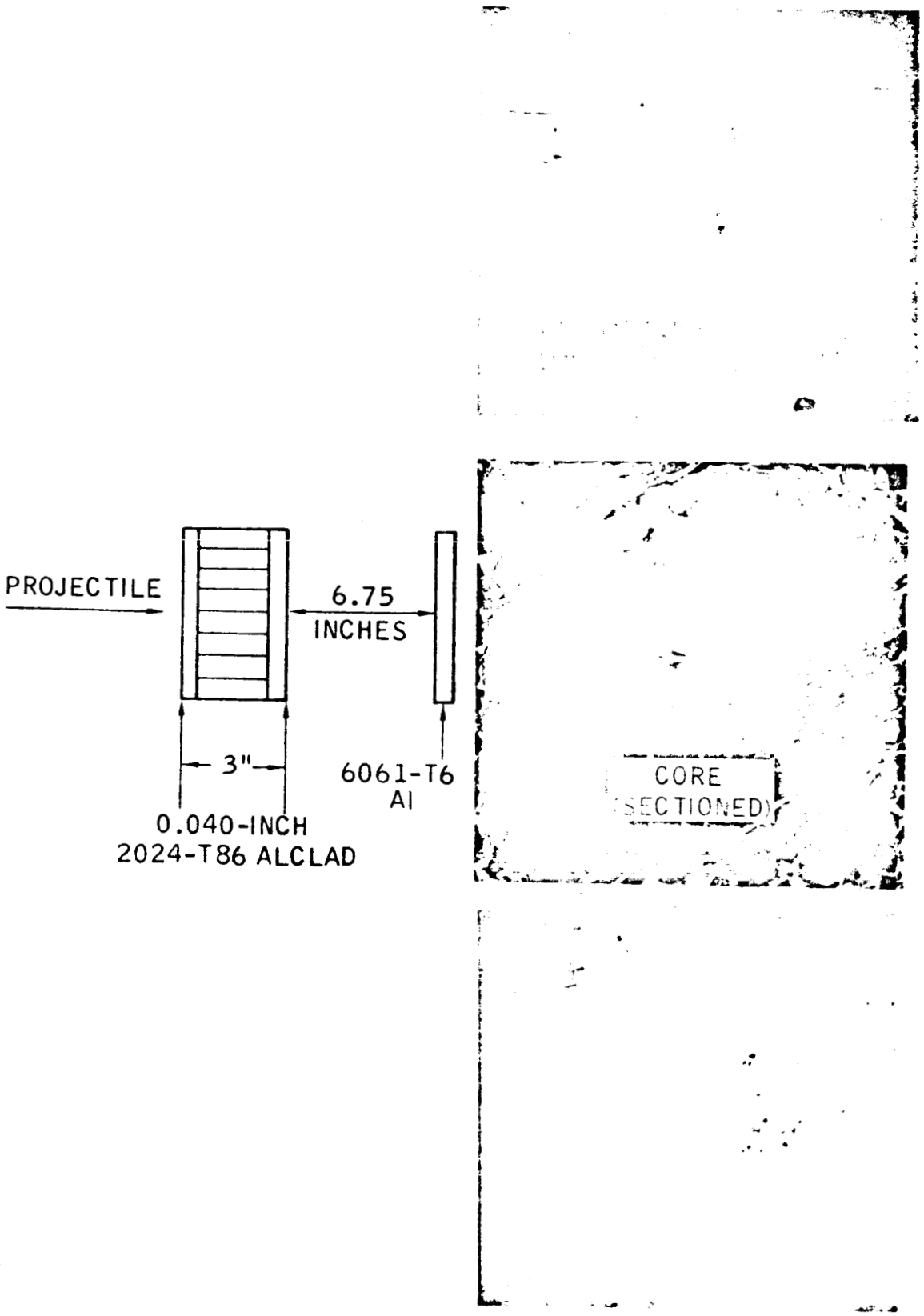

Figure 19. Honeycomb Panel No. 1

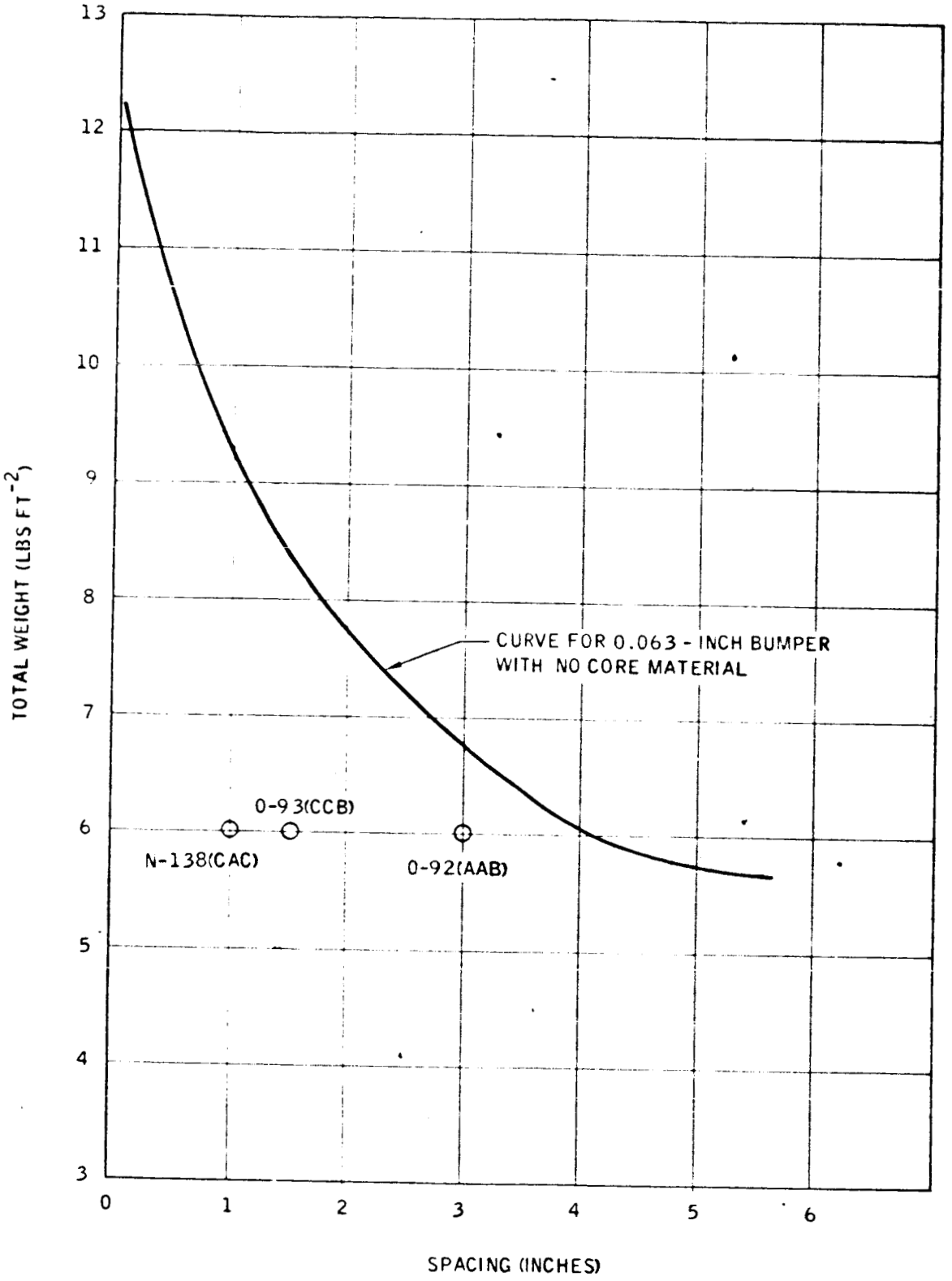

Figure 18. Fibrous Potassium Titanate Energy Absorber

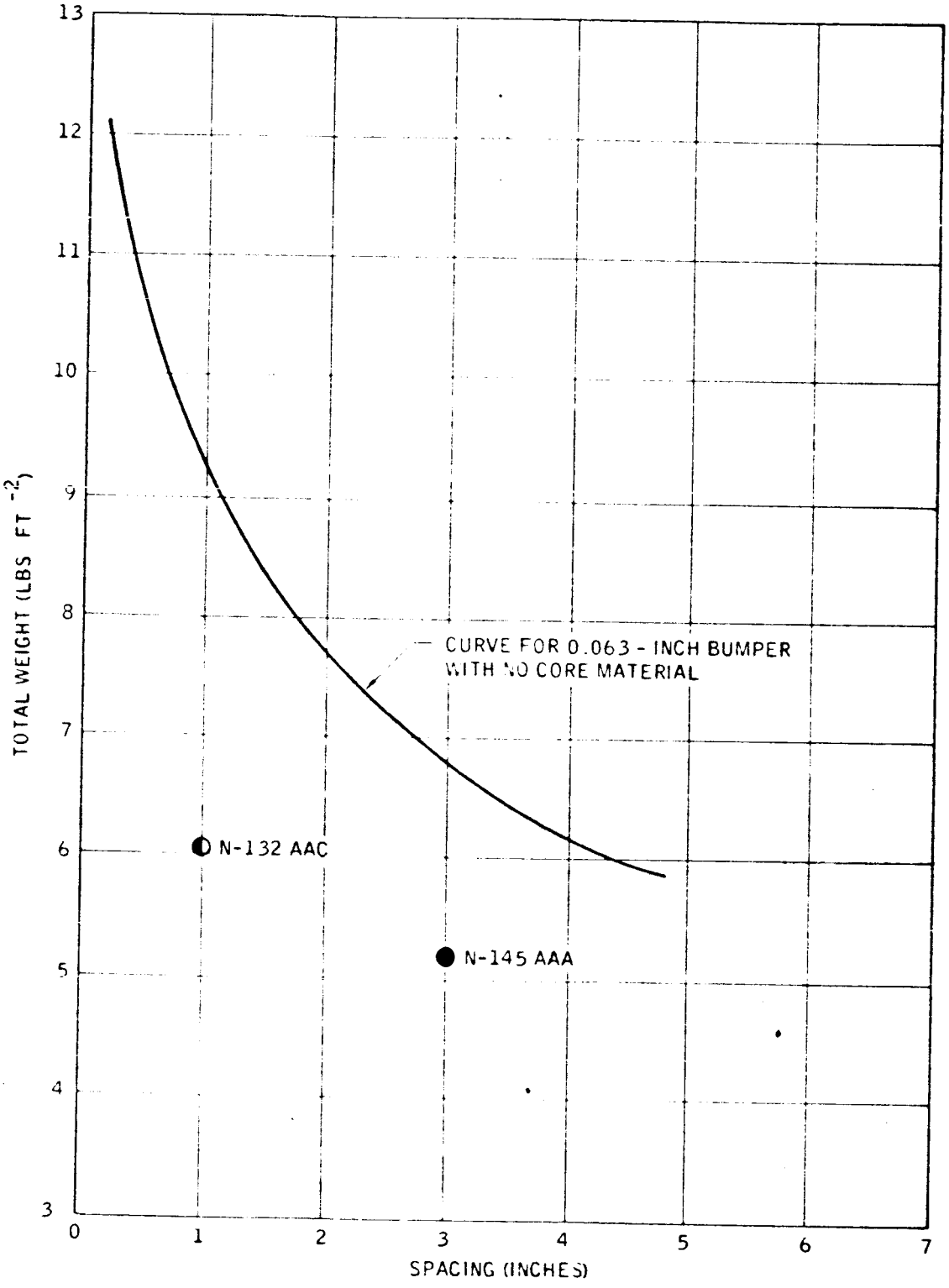

Figure 17. MIN K-1300 Energy Absorber

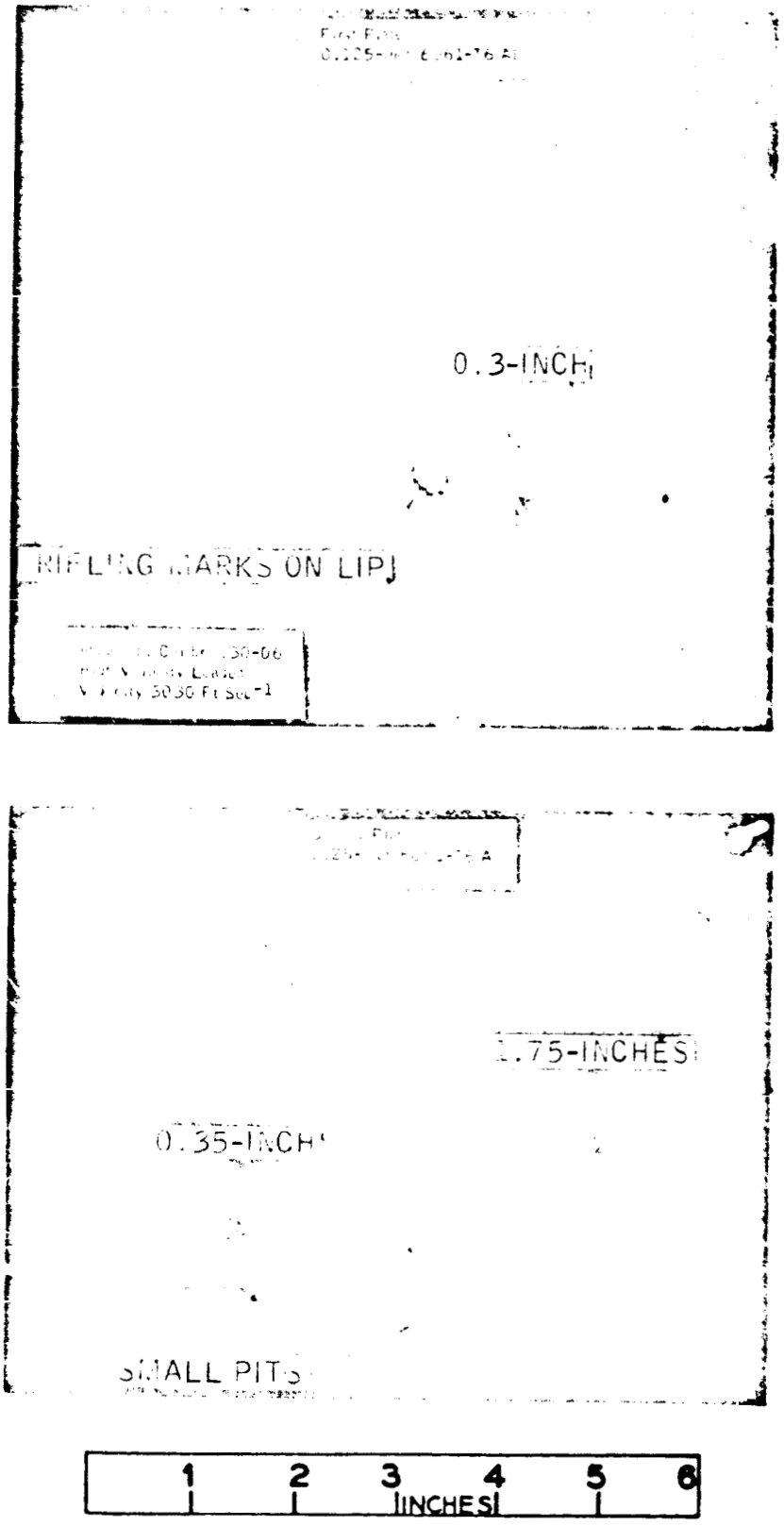

Figure 23. Damage to Aluminum Plates by a Caliber .30-06 Bullet

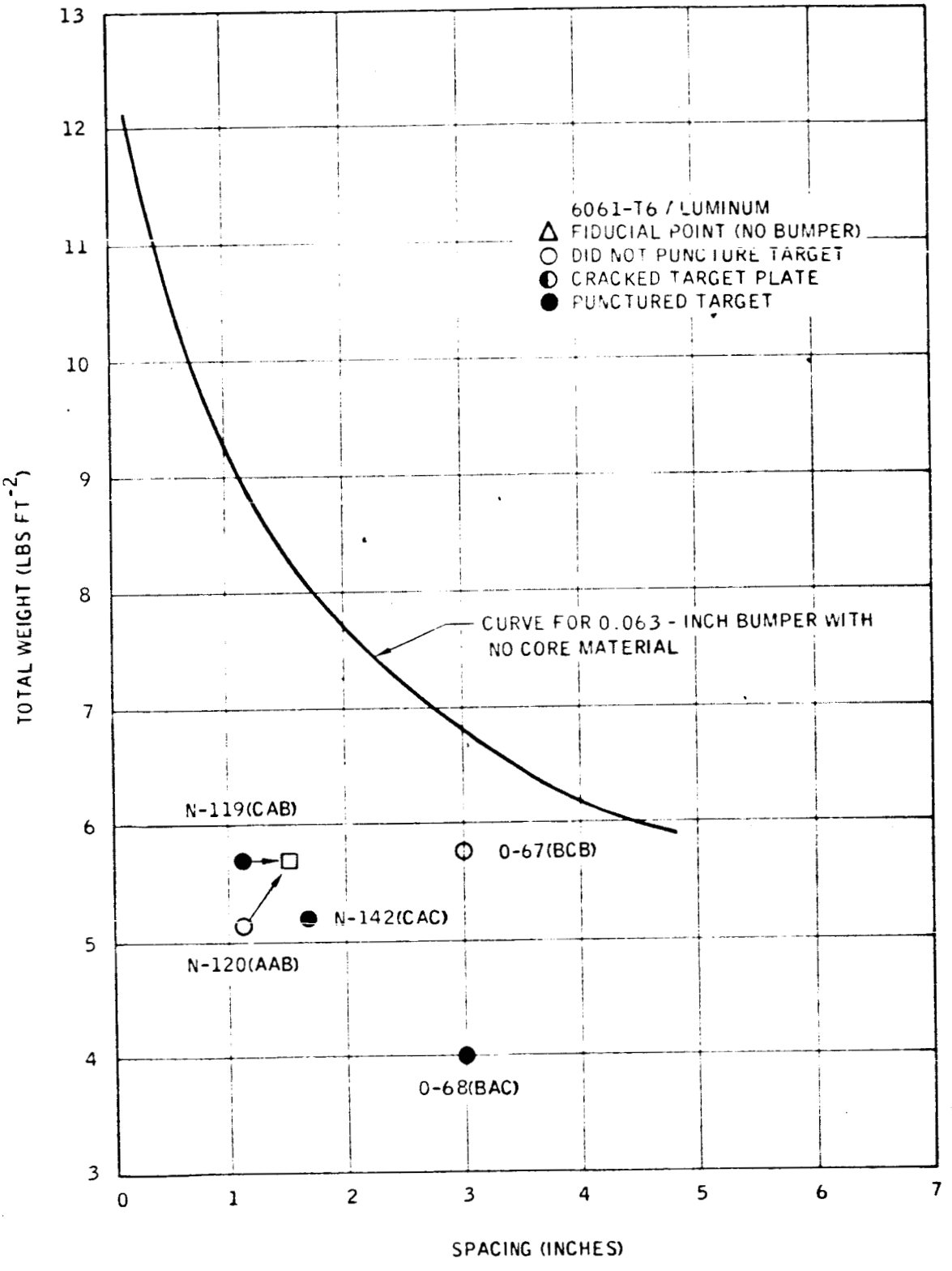

Figure 16. Fiberglas Energy Absorber

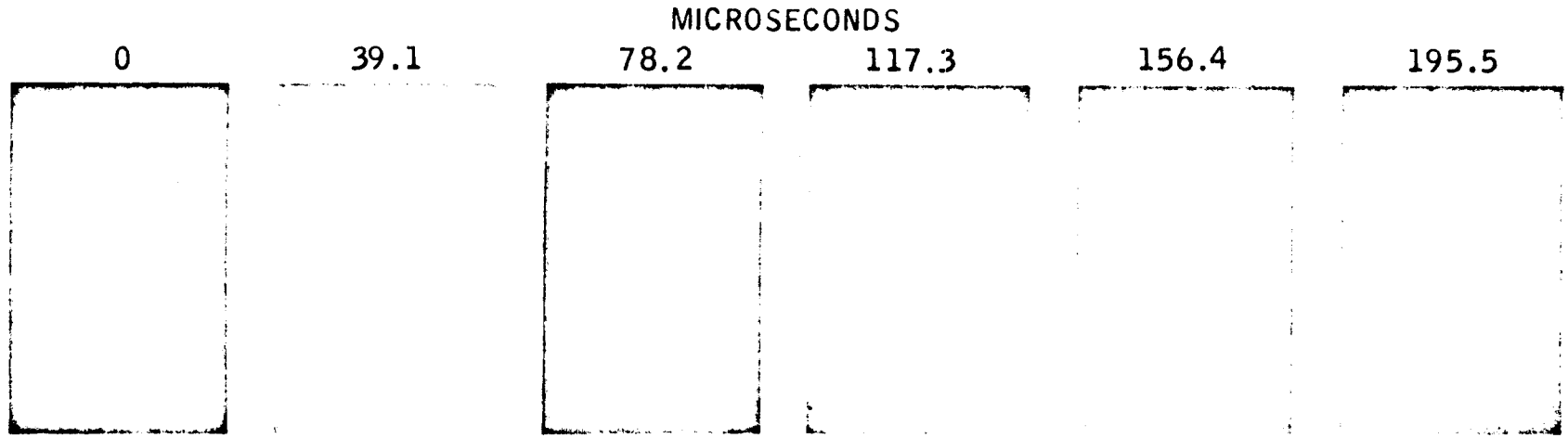

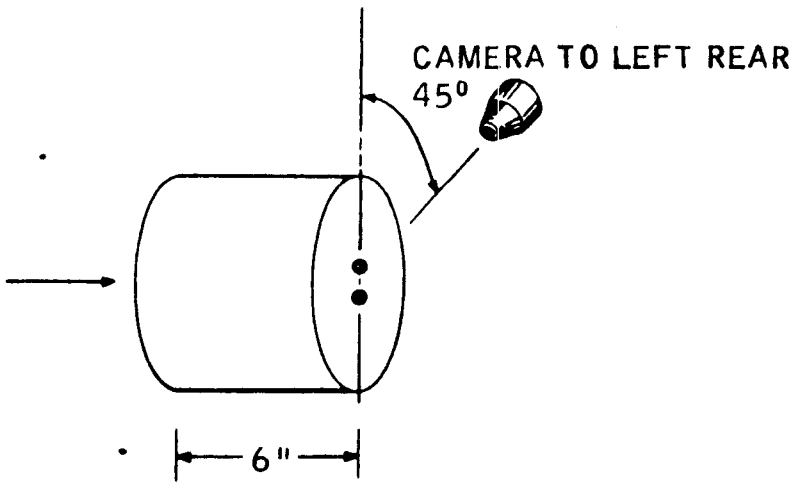

DIAPHRAGMS OF Ti-6Al-4V
0.016-INCH THICK
PROJECTILE
MASS, 0.097-GRAM
DIAMETER, 0.125-INCH
THICKNESS, 0.063-INCH
VELOCITY, 11,300 FT SEC^{-1}
25,600 FRAMES SEC^{-1}
DARK TIME: 39.1 ± 3.1 MICROSECONDS
EXPOSURE TIME: 1.0 MICROSECOND

AE62-0092

Figure 15. Burning of an Oxygen Pressurized Tank

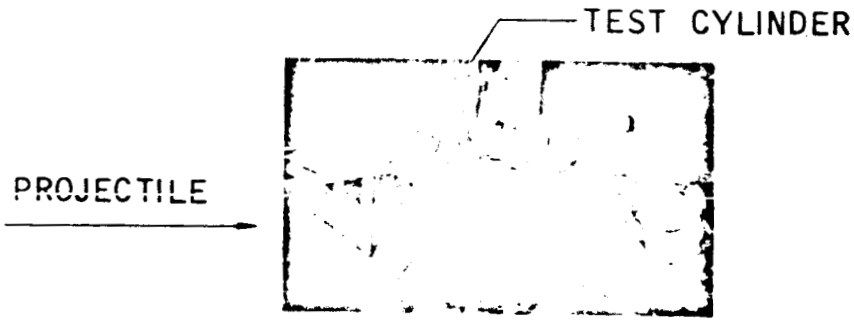

TEST ARRANGEMENT

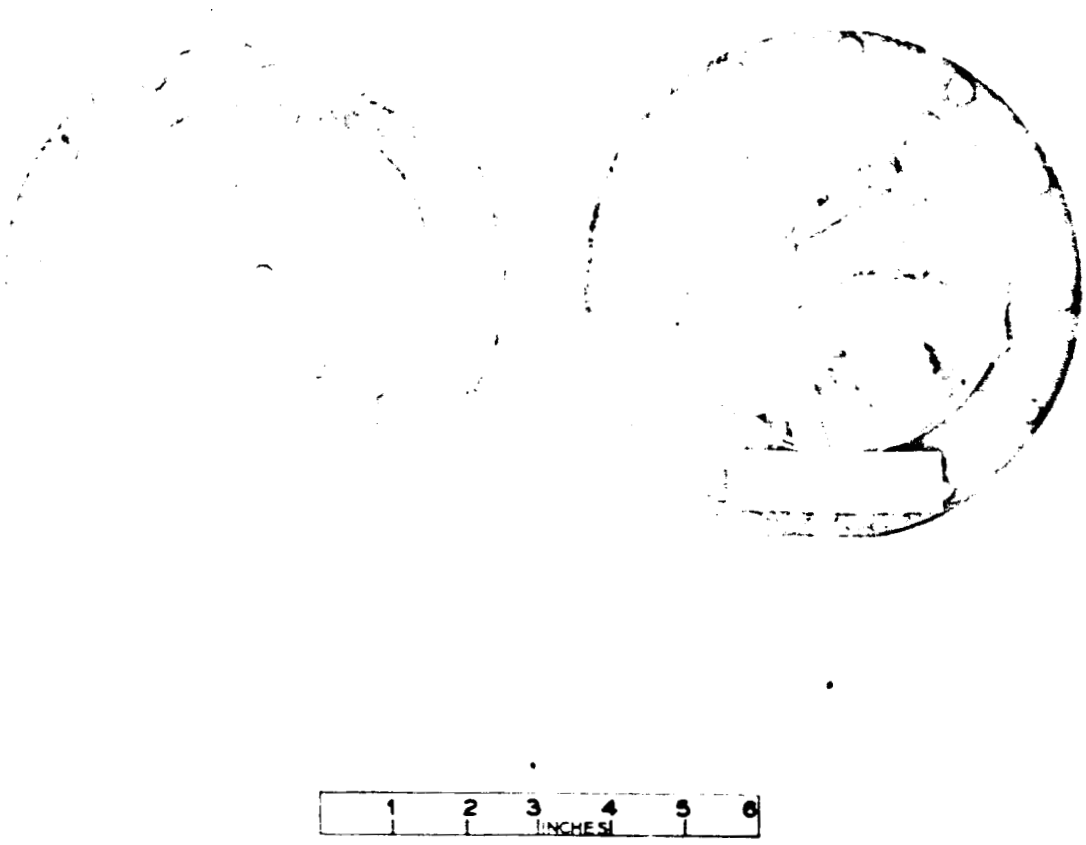

Figure 14. Oxygen Pressurized Tank: Test Panel No. 2

AE62-0092

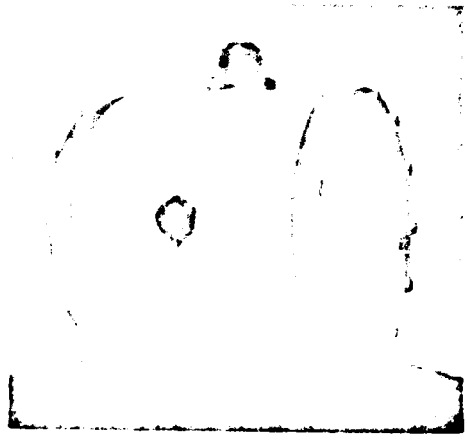

TEST PANEL

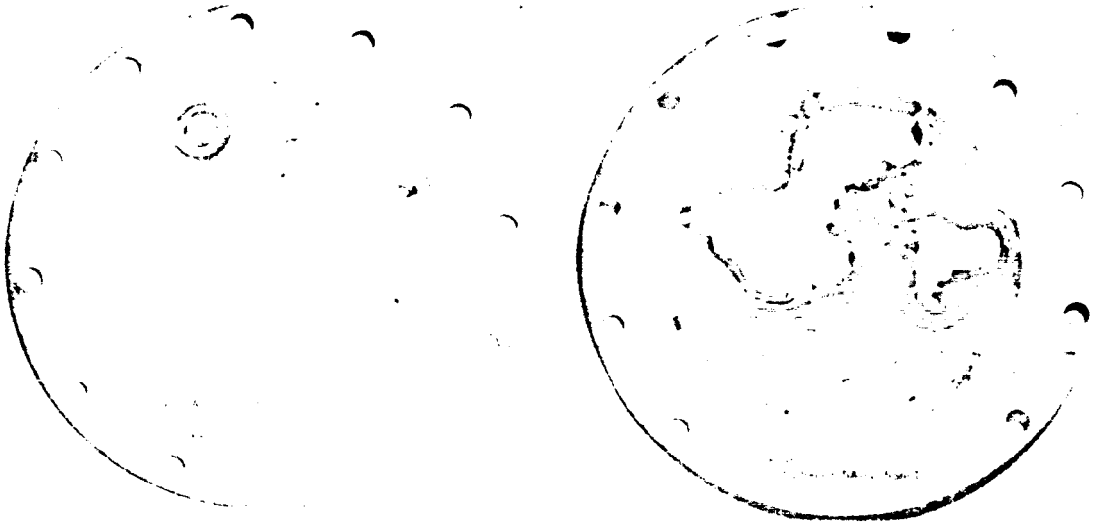

Figure 13. Oxygen Pressurized Tank: Test Panel No. 1

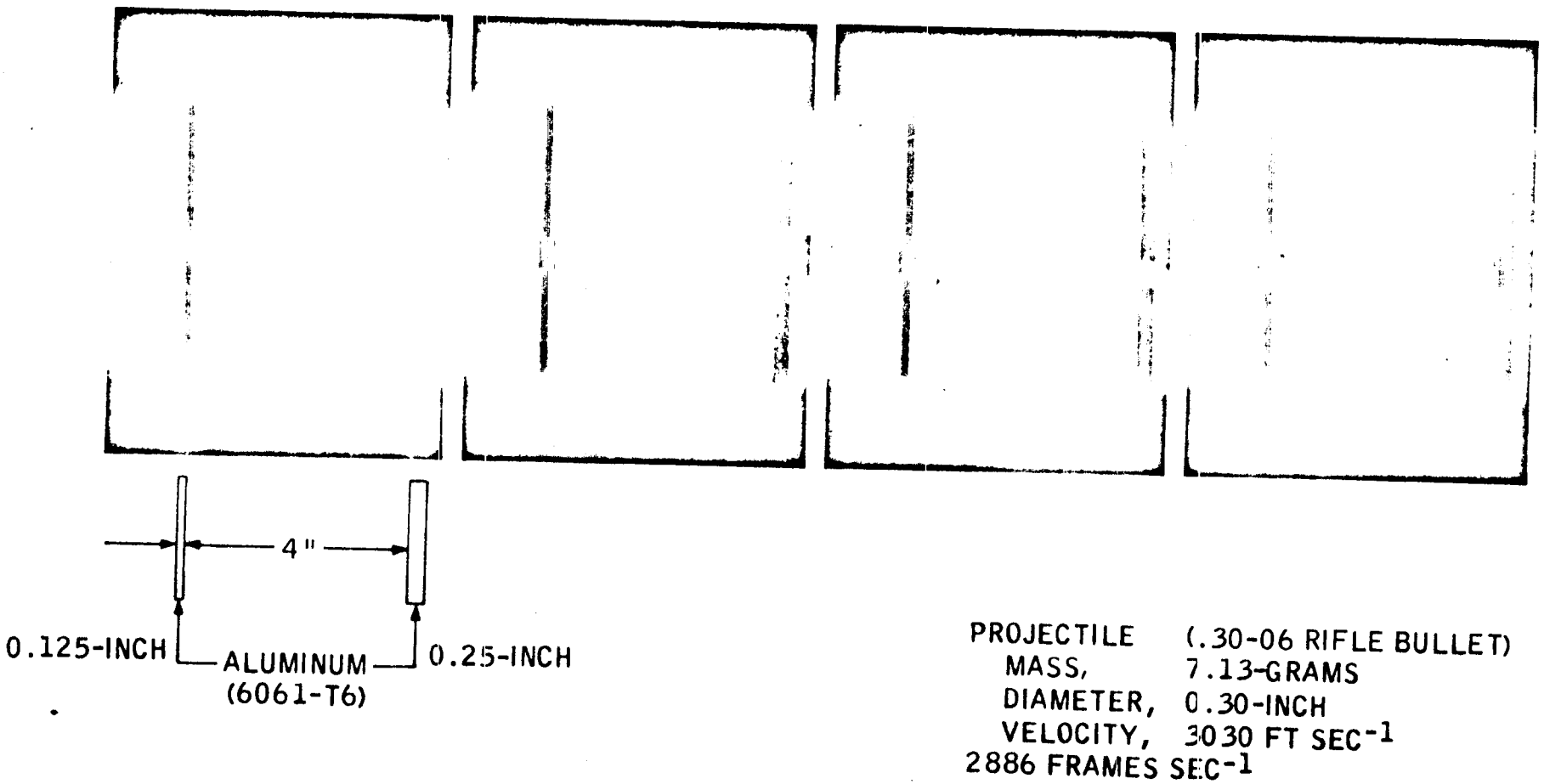

Figure 24. Slow Speed Impact Photographs

AE62-0092

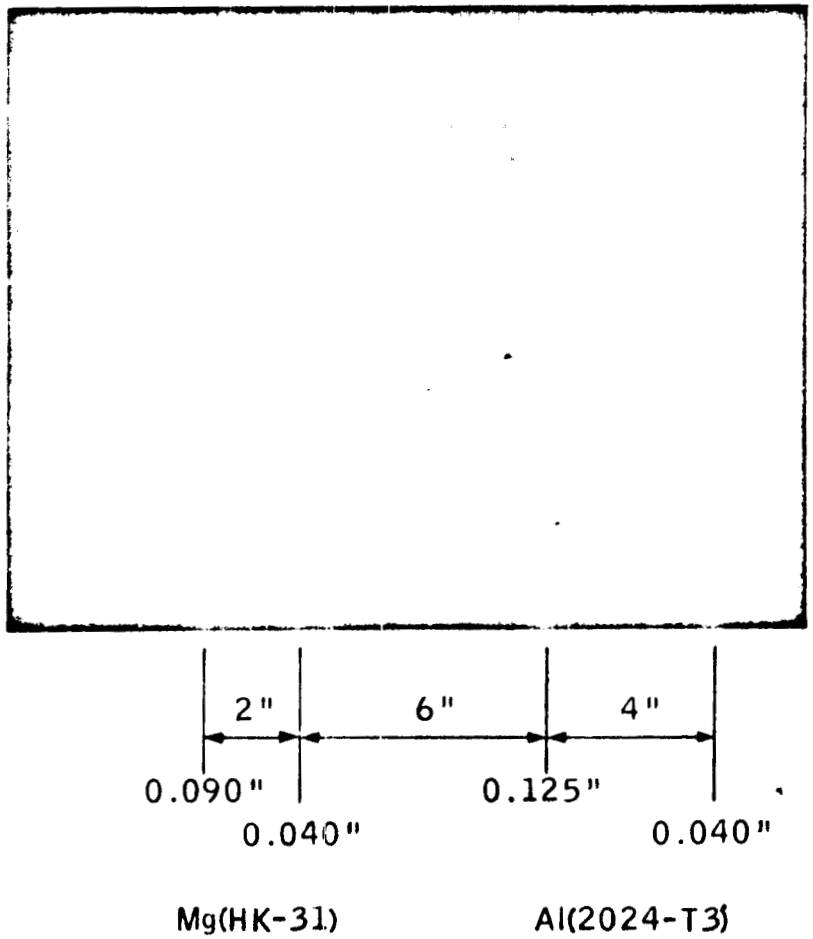

PROJECTILE
MASS, 0.55-GRAM
DIAMETER, 0.250-INCH
THICKNESS, 0.0938-INCH
VELOCITY, 15,800 FT SEC^{-1}

Figure 25. Impact Flash

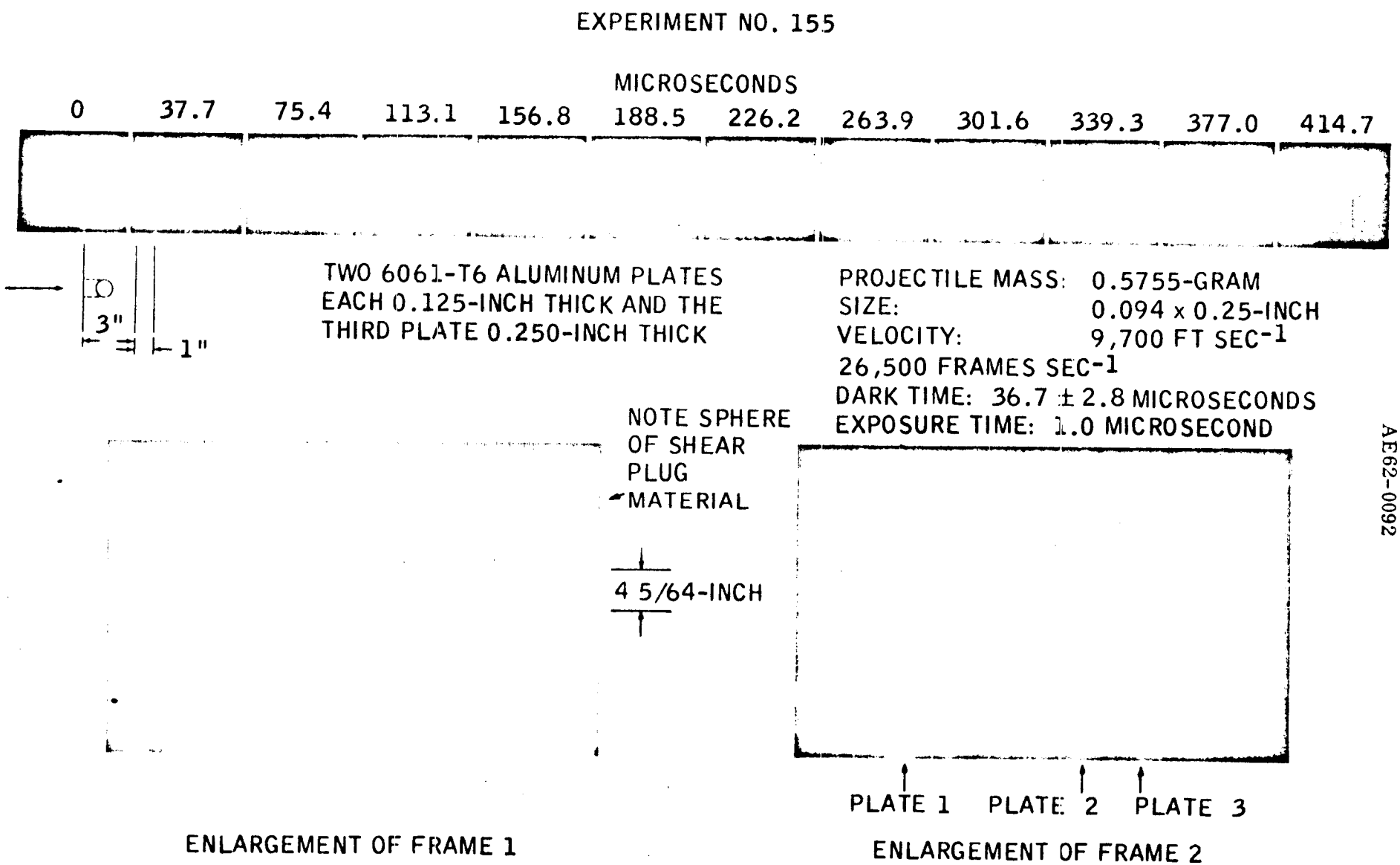

AE62-0092

Figure 26. Dynafax Photograph of Impact Phenomena Associated with Intermediate Speed Projectile

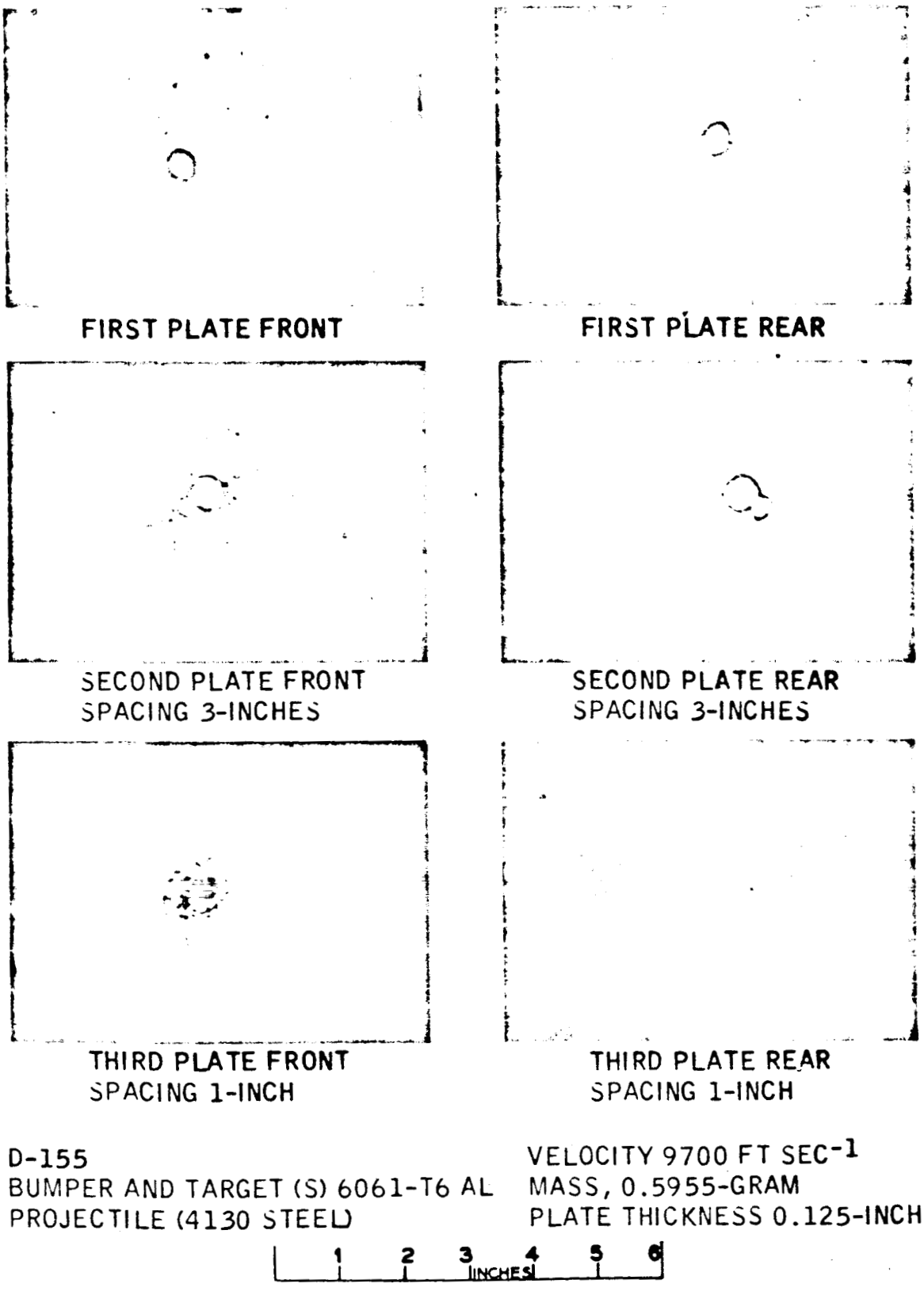

Figure 27. Aluminum Plates Used in Experiment D-155

EXPERIMENT NO. 157

FOUR 6061-T6 ALUMINUM PLATES EACH 0.125-INCH THICK

MICROSECONDS

0 38.8 77.6 116.4 155.2 194.0 232.8 271.6 310.4 349.2 388.0 426.8

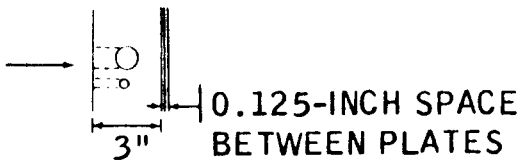

PROJECTILE
BROKE INTO
4 FRAGMENTS

PROJECTILE MASS: 0.5714-GRAM
SIZE: 0.094 x 0.25-INCH
VELOCITY: 28,600 FT SEC^{-1}
25,800 FRAMES SEC^{-1}
DARK TIME: 37.8 ± 3.0 MICROSECONDS
EXPOSURE TIME: 1.0 MICROSECOND

AE62-0092

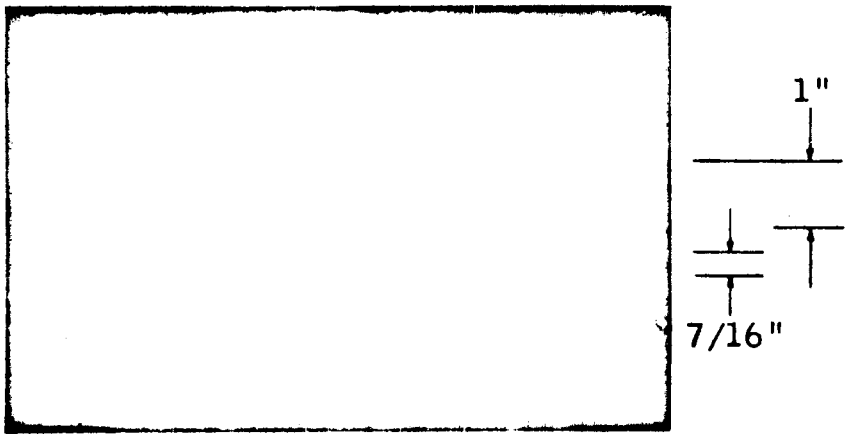

ENLARGEMENT OF FRAME 1
(Grids are Spaced One Inch Apart)

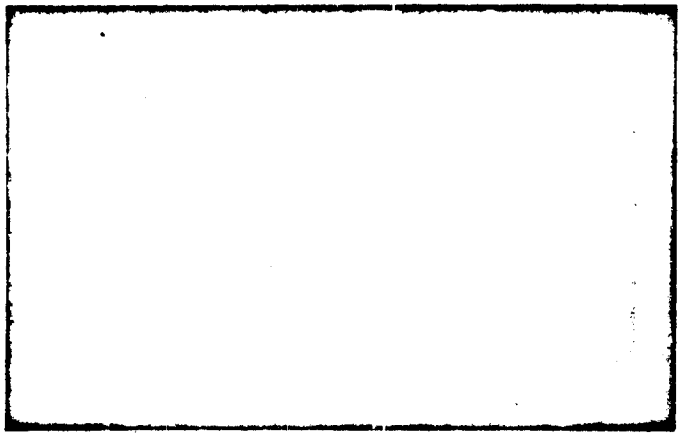

ENLARGEMENT OF FRAME 2

Figure 28. Dynafax Photograph of the Impact Phenomena Associated with a High Speed Projectile

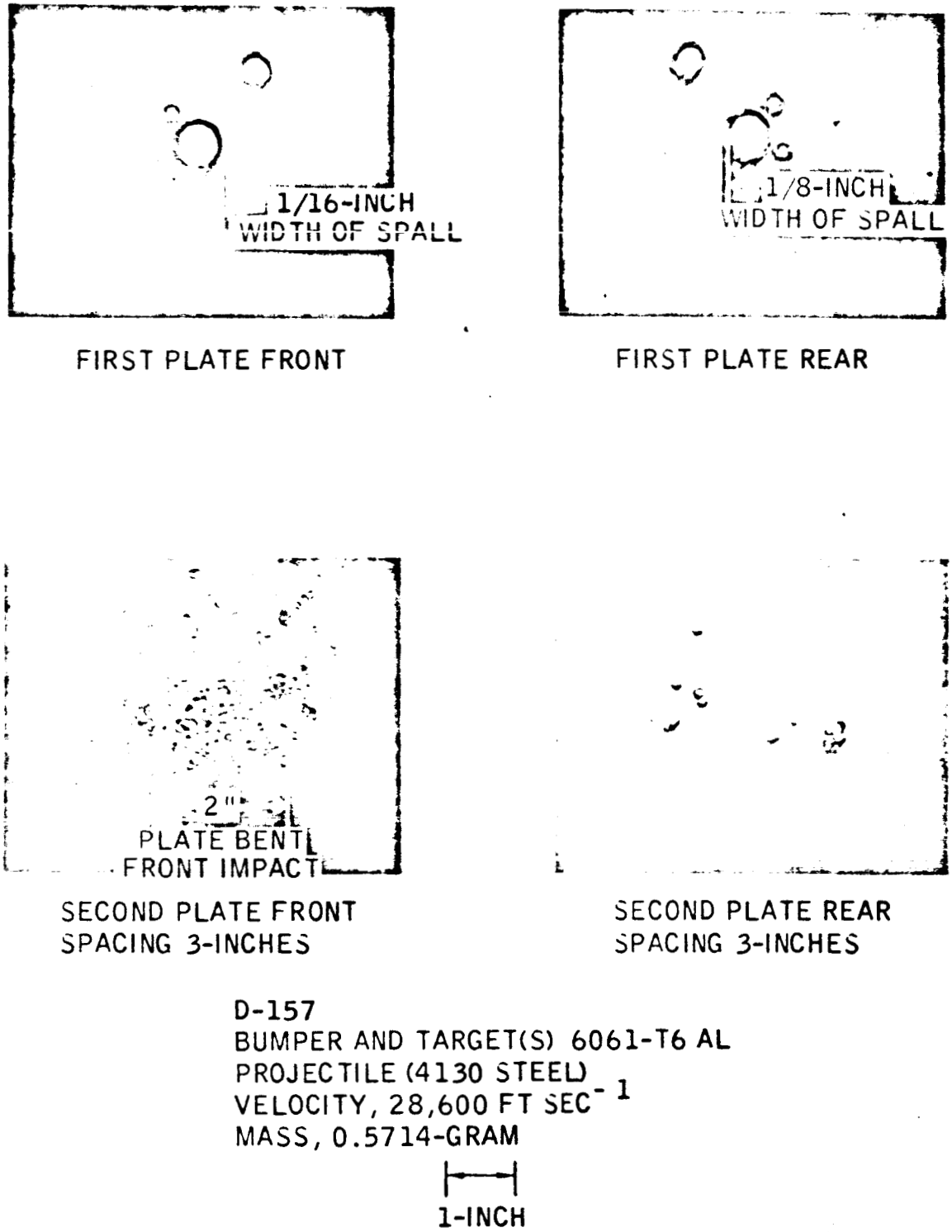

Figure 29. Aluminum Plates Used in Experiment D-157

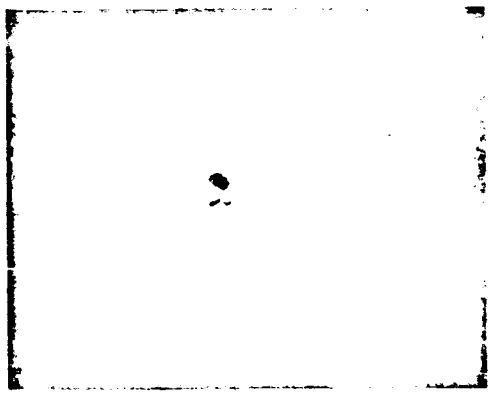

THIRD PLATE FRONT
SPACING 0.125-INCH

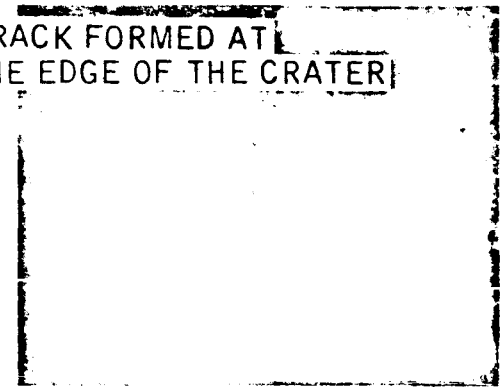

THIRD PLATE REAR
SPACING 0.125-INCH

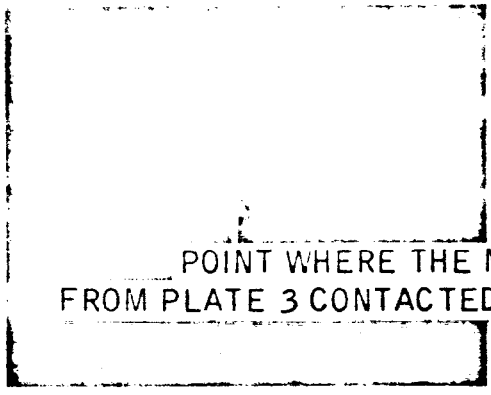

FOURTH PLATE FRONT
SPACING 0.125-INCH

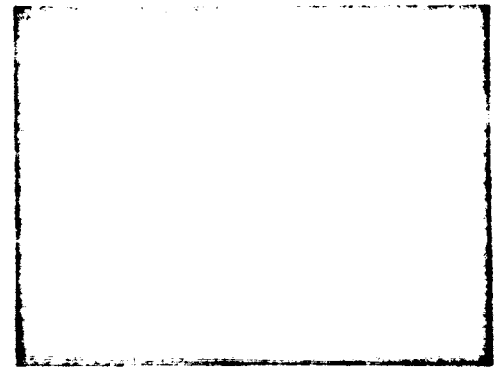

FOURTH PLATE REAR
SPACING 0.125-INCH

1-INCH

D-157
BUMPER AND TARGET(S) 6061-T6 Al.
PROJECTILE (4130 STEEL)
VELOCITY, 28,600 FT SEC^{-1}
MASS 0.5714 - GRAM

Figure 29A. Aluminum Plates Used in Experiment D-157

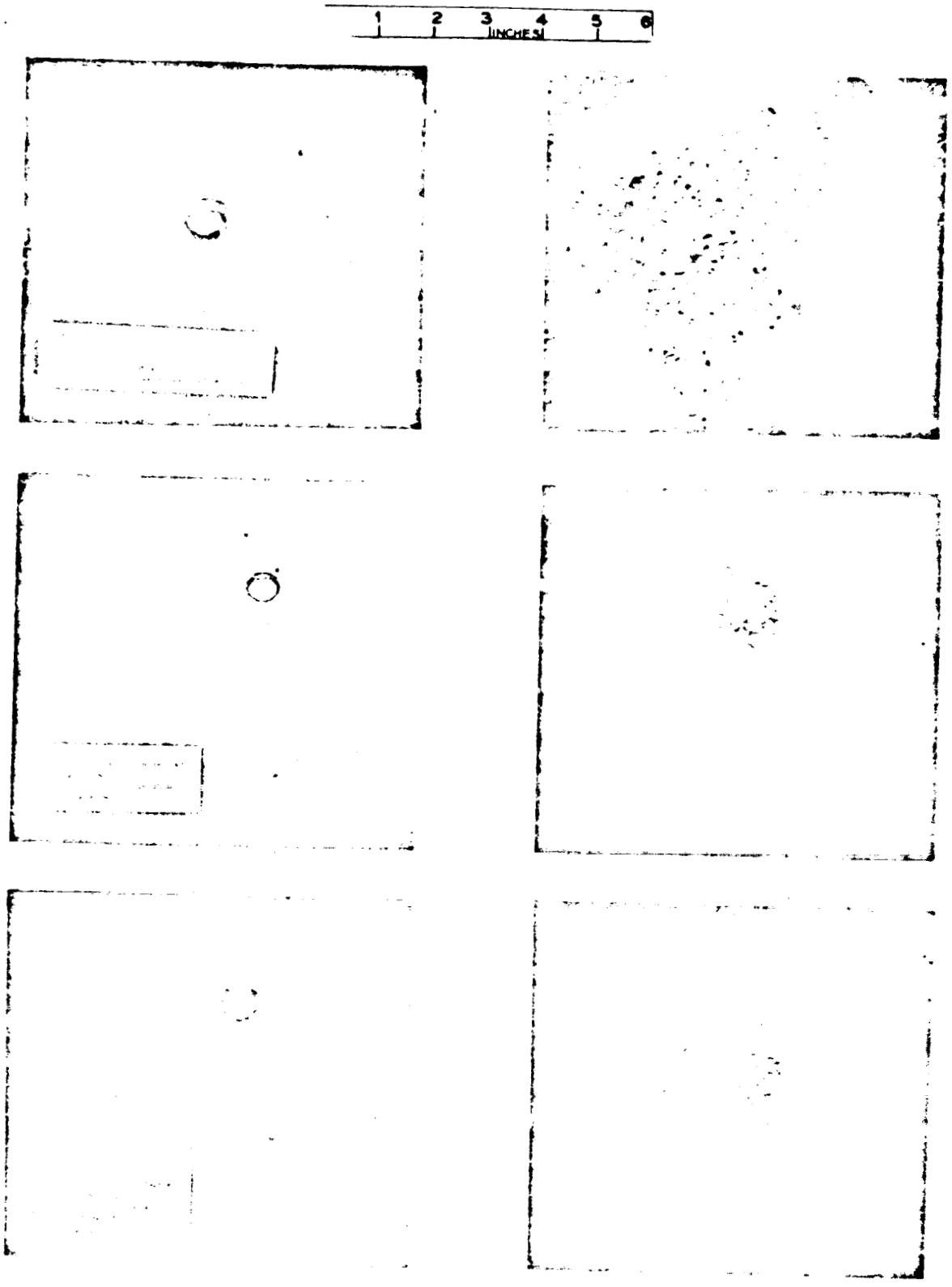

Figure 30. Projectile Behavior on Flat Face Impact

AE62-0092

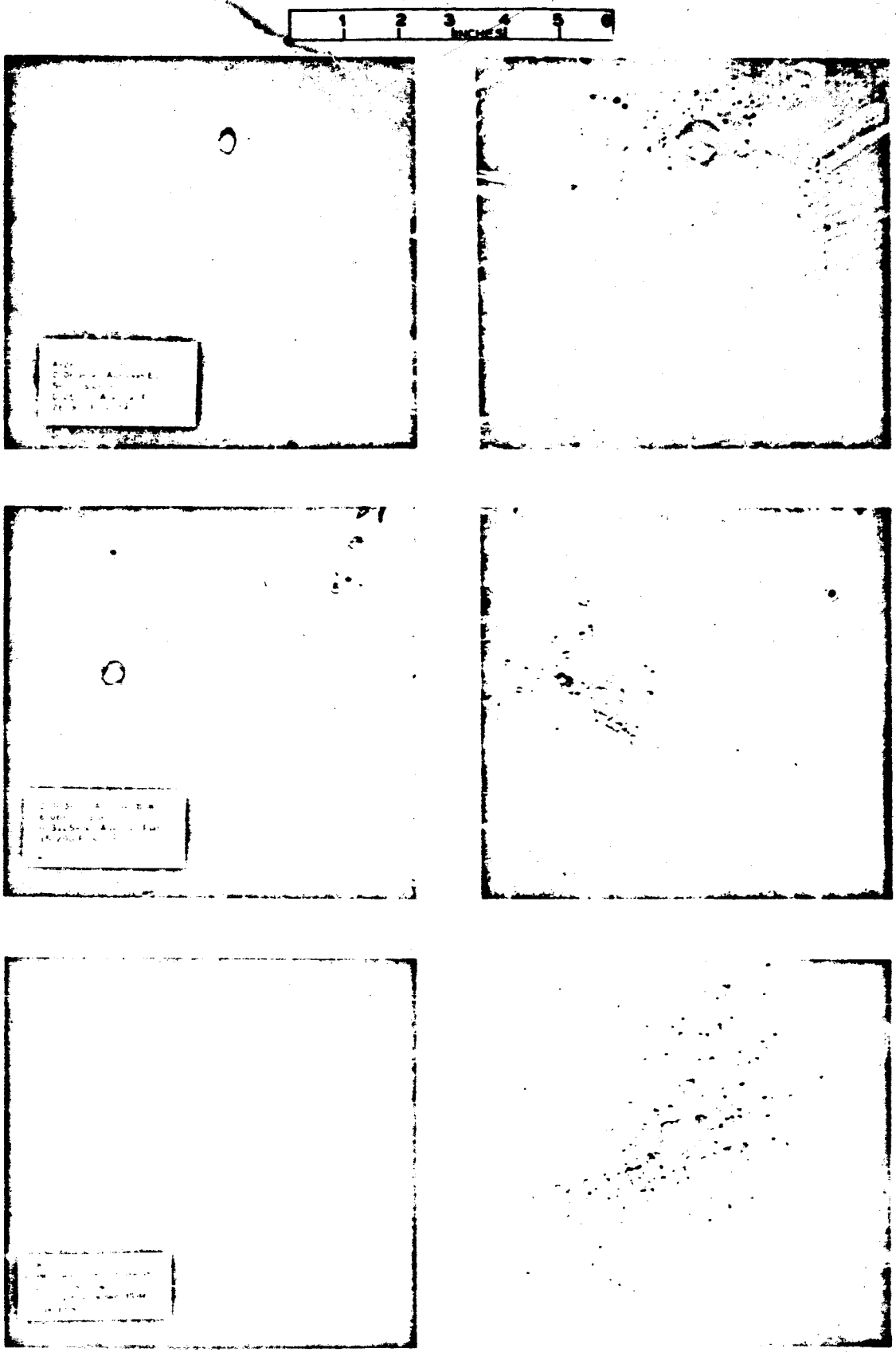

Figure 31. Projectile Behavior on Edge Impact